High c-Kit expression identifies hematopoietic stem cells with impaired self-renewal and megakaryocytic bias

Joseph Y. Shin,[1] Wenhuo Hu,[1] Mayumi Naramura,[4] and Christopher Y. Park[1,2,3]

[1]Human Oncology and Pathogenesis Program and [2]Department of Pathology and [3]Department of Laboratory Medicine, Memorial Sloan-Kettering Cancer Center, New York, NY 10065
[4]Eppley Institute for Research in Cancer and Allied Diseases, University of Nebraska Medical Center, Omaha, NE 68198

Hematopoietic stem cells (HSCs) are heterogeneous with respect to their self-renewal, lineage, and reconstitution potentials. Although c-Kit is required for HSC function, gain and loss-of-function c-Kit mutants suggest that even small changes in c-Kit signaling profoundly affect HSC function. Herein, we demonstrate that even the most rigorously defined HSCs can be separated into functionally distinct subsets based on c-Kit activity. Functional and transcriptome studies show HSCs with low levels of surface c-Kit expression (c-Kit^{lo}) and signaling exhibit enhanced self-renewal and long-term reconstitution potential compared with c-Kit^{hi} HSCs. Furthermore, c-Kit^{lo} and c-Kit^{hi} HSCs are hierarchically organized, with c-Kit^{hi} HSCs arising from c-Kit^{lo} HSCs. In addition, whereas c-Kit^{hi} HSCs give rise to long-term lymphomyeloid grafts, they exhibit an intrinsic megakaryocytic lineage bias. These functional differences between c-Kit^{lo} and c-Kit^{hi} HSCs persist even under conditions of stress hematopoiesis induced by 5-fluorouracil. Finally, our studies show that the transition from c-Kit^{lo} to c-Kit^{hi} HSC is negatively regulated by c-Cbl. Overall, these studies demonstrate that HSCs exhibiting enhanced self-renewal potential can be isolated based on c-Kit expression during both steady state and stress hematopoiesis. Moreover, they provide further evidence that the intrinsic functional heterogeneity previously described for HSCs extends to the megakaryocytic lineage.

CORRESPONDENCE
Christopher Y. Park:
parkc@mskcc.org

Abbreviations used: 5-FU, 5-fluorouracil; HSC, hematopoietic stem cell; MkP, megakaryocyte progenitor; L$^-$S$^+$K$^+$, Lin$^-$ Sca-1$^+$ c-Kit$^+$; SCF, stem cell factor.

Mature hematopoietic cells develop from hematopoietic stem cells (HSCs) through a hierarchically organized process that produces increasingly lineage-restricted cells with decreasing self-renewing capacity (Bryder et al., 2006). Although HSCs and committed progenitors possess the ability to mature into multiple hematopoietic lineages, HSCs are unique in their long-term self-renewal capacity, which is highly associated with their relative quiescent nature (Wilson et al., 2008; Foudi et al., 2009; van der Wath et al., 2009). Previous studies have identified numerous cell-intrinsic factors involved in regulating HSC function, including the cell surface protein tyrosine kinase c-Kit, which interacts with its cognate ligand, stem cell factor (SCF), to regulate HSC self-renewal (Sharma et al., 2007; Thorén et al., 2008; Waskow et al., 2009; Wilson et al., 2009).

c-Kit signaling plays a critical role in regulating HSC function. For instance, mice harboring loss-of-function mutations in c-Kit exhibited reductions in HSC number and CFU-spleen (McCulloch et al., 1964; Yee et al., 1994; Miller et al., 1996). In vivo treatment of mice with an anti–c-Kit monoclonal antibody (ACK2) that blocks the interaction between c-Kit and SCF promoted clearance of HSCs from the bone marrow, supporting the critical role of c-Kit–SCF interactions in promoting HSC self-renewal (Shiohara et al., 1993; Czechowicz et al., 2007). In contrast, mice bearing *c-kit* gain-of-function mutations exhibited a marked expansion of myeloid cells compatible with a myeloproliferative disorder (Bosbach et al., 2012). Also, mice with loss-of-function mutations of *c-Cbl*, an E3 ubiquitin

The Rockefeller University Press $30.00
J. Exp. Med. 2014 Vol. 211 No. 2 217-231
www.jem.org/cgi/doi/10.1084/jem.20131128

The Journal of Experimental Medicine

ligase that produces a negative feedback response to c-Kit signaling, exhibited a mild myeloproliferative disorder (Zeng et al., 2005; Masson et al., 2006; Rathinam et al., 2008), underscoring the consequences of constitutive c-Kit signaling on HSC/progenitor proliferation and/or commitment. Collectively, these findings indicate that marked alterations in c-Kit signaling result in dramatic HSC phenotypes, but it is not clear whether the variation in c-Kit activity in normal HSCs results in varying functional consequences for HSCs.

Advances in cell sorting techniques have enabled the purification of HSCs to near homogeneity such that 10 out of 13 of these cells can long-term reconstitute myeloablated mice at a single-cell level (Lineage$^-$ c-Kit$^+$ Sca-1$^+$ CD150$^+$ CD34$^-$; (Morita et al., 2010)). Additionally, HSC populations negative for Flk2, CD48, and CD41 or low in rhodamine staining are further enriched for self-renewing cells (Christensen and Weissman, 2001; Kiel et al., 2005; Weksberg et al., 2008). Genetic tracing and single-cell HSC transplants have shown that immunophenotypically defined populations of HSCs are functionally heterogeneous, differing with respect to various properties including cell cycling status, engraftment capacity, lineage bias, and self-renewal potential (Müller-Sieburg et al., 2002; Dykstra et al., 2007; Gerrits et al., 2010). These findings underscore the need for improving methods to prospectively isolate functionally distinct HSC subtypes to better characterize the molecular basis of their differences.

Highly purified normal HSCs (Lineage$^-$ c-Kit$^+$ Sca-1$^+$ CD150$^+$ CD34$^-$ Flk2$^-$ CD48$^-$ CD41$^-$) express a log-fold range in cell surface c-Kit levels. Given the importance of c-Kit signaling in HSC maintenance and the dramatic phenotypes induced when the pathway is perturbed, we hypothesized that differences in c-Kit signaling would result in differential HSC function and identify functionally distinct classes of HSCs. Our data indicate that even the most enriched HSC populations can be fractionated based on cell surface c-Kit expression levels, with c-Kit^{lo} HSCs exhibiting enhanced self-renewal and long-term reconstitution potential compared with c-Kit^{hi} HSCs. Functional studies both in vitro and in vivo demonstrate that HSCs with higher levels of c-Kit signaling preferentially differentiate into megakaryocytes, a previously unappreciated lineage bias found within the purest HSCs. We also show that the ability of c-Kit expression levels to distinguish these HSC subtypes is preserved even in the context of bone marrow insult, indicating that c-Kit signaling is not stochastic, but instead represents a precisely regulated signaling pathway required for physiologically appropriate HSC function. Finally, we show that the transition from c-Kit^{lo} to c-Kit^{hi} HSCs is negatively regulated by c-Cbl, an E3 ubiquitin ligase, to ensure proper control over the composition of functionally distinct HSC subtypes.

RESULTS

Expansion potential and proliferation of HSCs vary based on c-Kit levels

To determine whether differential expression of c-Kit on HSCs can identify functionally distinct HSCs (Lineage$^-$ c-Kit$^+$ Sca-1$^+$ CD150$^+$ CD34$^-$), we assessed the proliferative capacity and colony-forming ability of 100 double FACS-sorted c-Kit^{hi} and c-Kit^{lo} HSCs seeded into cytokine-supplemented liquid cultures or methylcellulose media. To obtain pure and distinct populations of HSCs, we gated the top 30% and bottom 30% of c-Kit expressors (Fig. 1 A and Fig. S1). After 7 d, mature hematopoietic cell output and colony types were evaluated. In liquid culture, c-Kit^{hi} HSCs produced 6.5-fold more cells than c-Kit^{lo} HSCs (Fig. 1 B; $P < 0.01$). To confirm the difference in the cell division kinetics of c-Kit^{hi} and c-Kit^{lo} HSCs, we used HSCs isolated from mice expressing tetracycline-inducible GFP-labeled histone 2B (TetOP-H2B-GFP), which allows the monitoring of cell division kinetics by measuring the rate of GFP dilution by flow cytometry (Foudi et al., 2009). 1,200 c-Kit^{hi} and c-Kit^{lo} HSCs from doxycycline-treated TetOP-H2B-GFP mice were sorted into doxycycline-free media supplemented with complete cytokines. After 5 d of culture, c-Kit^{hi} HSCs expressed 2.3-fold lower mean fluorescence intensity (MFI) of GFP than c-Kit^{lo} HSCs (Fig. 1, C and D).

We next evaluated the differentiation kinetics and colony-forming ability of c-Kit^{lo} and c-Kit^{hi} HSCs. After 5 d in cytokine-supplemented liquid culture, c-Kit^{hi} HSCs produced 3.3-fold more Lin$^-$Sca-1$^-$c-Kit$^+$ (L$^-$S$^-$K$^+$) myeloid progenitors and 1.9-fold fewer Lin$^-$ Sca-1$^+$ c-Kit$^+$ (L$^-$S$^+$K$^+$) cells compared with c-Kit^{lo} HSCs ($P = 0.0073$ and 0.02, respectively; Fig. 1 E), suggesting that c-Kit^{hi} HSCs differentiate more rapidly than c-Kit^{lo} HSCs. Although c-Kit^{hi} and c-Kit^{lo} HSCs produced comparable frequencies of early myeloid/erythroid precursors such as pregranulocyte-macrophage precursors (preGM) and preCFU erythroid precursors (preCFUe; not depicted), c-Kit^{hi} HSCs produced higher frequencies of precursors with megakaryocytic potential, including 1.5-fold more premegakaryocyte/erythroid progenitors (preMegE) in addition to 2.4-fold more committed megakaryocyte progenitors (MkP; Fig. 1 F; Pronk et al., 2007). Consistent with more rapid differentiation kinetics of c-Kit^{hi} HSCs, c-Kit^{hi} HSCs produced 3.7-fold more colonies than c-Kit^{lo} HSCs after 7 d in methylcellulose media ($P < 0.01$; Fig. 1 G), but after 14 d c-Kit^{hi} HSCs produced 1.3-fold fewer colonies. Furthermore, c-Kit^{hi} HSCs produced 1.7-fold more colonies derived from lineage-restricted progenitors (CFU-GM, CFU-G, and CFU-M), but 3.3-fold fewer colonies from multipotent progenitors (CFU-GEMM; Fig. 1 H). When 100,000 cells from the primary methylcellulose cultures were secondarily plated, c-Kit^{lo} HSCs produced 5.3-fold more colonies than c-Kit^{hi} HSCs ($P < 0.05$; Fig. 1 G). These results show that c-Kit^{hi} HSCs proliferate and terminally differentiate more rapidly than c-Kit^{lo} HSCs and exhibit reduced replating efficiency. Consistent with these studies, c-Kit^{hi} HSCs from freshly isolated, wild-type bone marrow showed evidence of increased cell cycling and were 2.4-fold enriched for cells in the G2/S/M phases of the cell cycle in comparison to c-Kit^{lo} HSCs ($P = 0.001$; Fig. 1 I). Together, these data indicate that c-Kit^{hi} HSCs proliferate and differentiate more rapidly than c-Kit^{lo} HSCs and that they preferentially adopt megakaryocytic fates.

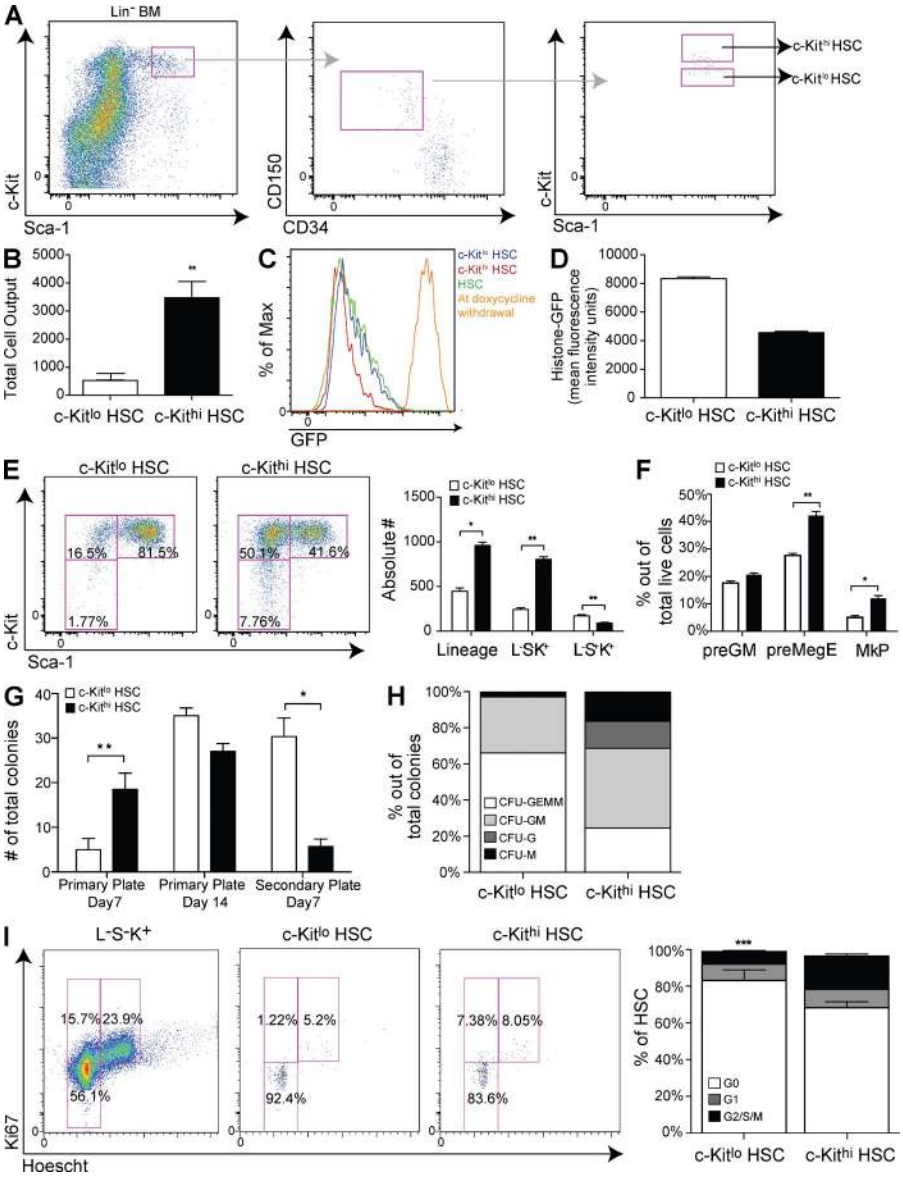

Figure 1. Differential expression of c-Kit subdivides HSCs into distinct populations. (A) c-Kit^{hi} and c-Kit^{lo} HSCs were defined as the top 30% or lowest 30% of c-Kit expressors, respectively, among immunophenotypically defined HSCs (Lin$^-$ c-Kit$^+$ Sca-1$^+$ SLAM$^+$ CD34$^-$). (B) c-Kit^{hi} and c-Kit^{lo} HSCs were double FACS-sorted into liquid culture media supplemented with differentiation-inducing cytokines. After 5 d in culture, total cell output was quantified using a hemocytometer. (C) TetOP-H2B.GFP mice were given doxycycline-treated water for 6 wk before experimentation. 100 TetOP-H2B.GFP$^+$ c-Kit^{hi} or c-Kit^{lo} HSCs were double FACS-sorted into cytokine supplemented liquid culture. After 5 d, label retention by c-Kit$^+$ (green), c-Kit^{lo} (blue), and c-Kit^{hi} (red) HSCs was measured by flow cytometry. (D) The GFP mean fluorescence intensity (MFI) in c-Kit^{lo} and c-Kit^{hi} HSCs was quantified. (E) Differentiation kinetics were assessed by determining the cellular composition of progeny derived from HSCs using flow cytometry after 5 d in liquid culture. (F) Development of mature progenitors by C57BL/6 c-Kit^{hi} and c-Kit^{lo} HSCs was assessed by flow cytometry after 5 d in culture (preGM, L$^-$S$^-$K$^+$ CD41$^-$ CD16/32$^-$ CD105$^-$ CD150$^-$; preCFUe, L$^-$S$^-$K$^+$ CD41$^-$ CD16/32$^-$ CD105$^+$ CD150$^+$; preMegE, L$^-$S$^-$K$^+$ CD41$^-$ CD16/32$^-$ CD105$^-$ CD150$^+$; MkP, L$^-$S$^-$K$^+$ CD41$^+$ CD150$^+$). (G) 100 c-Kit^{hi} and c-Kit^{lo} HSCs were double FACS-sorted into cytokine supplemented methylcellulose media, and total colony output was scored at indicated time points. After 14 d of primary culture, 100,000 cells from each culture were replated into fresh methylcellulose media. (H) Colony types were scored in primary and secondary colony assays after 14 d in culture. (I) Cell cycle analysis of freshly isolated bone marrow was performed using Ki67 and Hoechst 33342, and positive gates were drawn based on isotype controls. Results are representative of three independent experiments, and shown as mean ± SEM. n = 4–5 mice. *, P < 0.05; **, P < 0.01; ***, P < 0.0001.

c-Kit^{hi} HSCs exhibit poor engraftment potential

Given the correlation between HSC function and quiescence, we hypothesized that the more proliferative c-Kit^{hi} HSCs would exhibit poorer reconstitution potential than c-Kit^{lo} HSCs (Glimm et al., 2000; Passegué et al., 2005; Wilson et al., 2008; Foudi et al., 2009; van der Wath et al., 2009; Pietras et al., 2011). To characterize the engraftment potential of c-Kit^{hi} and c-Kit^{lo} HSCs, 400 cells of each HSC subset (CD45.2$^+$) were competitively transplanted with 300,000 competitor bone marrow cells (CD45.1$^+$) into lethally irradiated, congenic recipients (CD45.1$^+$). Peripheral blood chimerism levels were assessed each week after transplantation. Mice transplanted with c-Kit^{lo} and c-Kit^{hi} HSCs exhibited comparable total CD45 chimerism levels in the peripheral blood up to 4 wk after transplant (Fig. 2, A–D). However, whereas mice transplanted with c-Kit^{lo} HSCs exhibited increasing peripheral blood donor CD45 chimerism levels from 4 to 16 wk after transplant (34.9–78.8%), c-Kit^{hi} HSC-transplanted mice did not exhibit a significant increase in chimerism during the same time period (30.7–21.6%). By week 16 after transplant, chimerism levels of all lineages were significantly lower in mice transplanted with c-Kit^{hi} HSCs compared with c-Kit^{lo} HSC-transplanted mice (B cells: 23.89 vs. 80.97%, P = 0.0003; T cells: 18.22 vs. 59.54%, P = 0.0007; granulocytes: 18.01 vs. 83.99%, P < 0.0001), consistent with a long-term engraftment defect.

Although peripheral blood granulocyte chimerism is generally considered a good indicator of HSC chimerism, it is not clear whether fractionating HSCs based on c-Kit expression might enrich for lineage-biased HSCs, thereby providing a

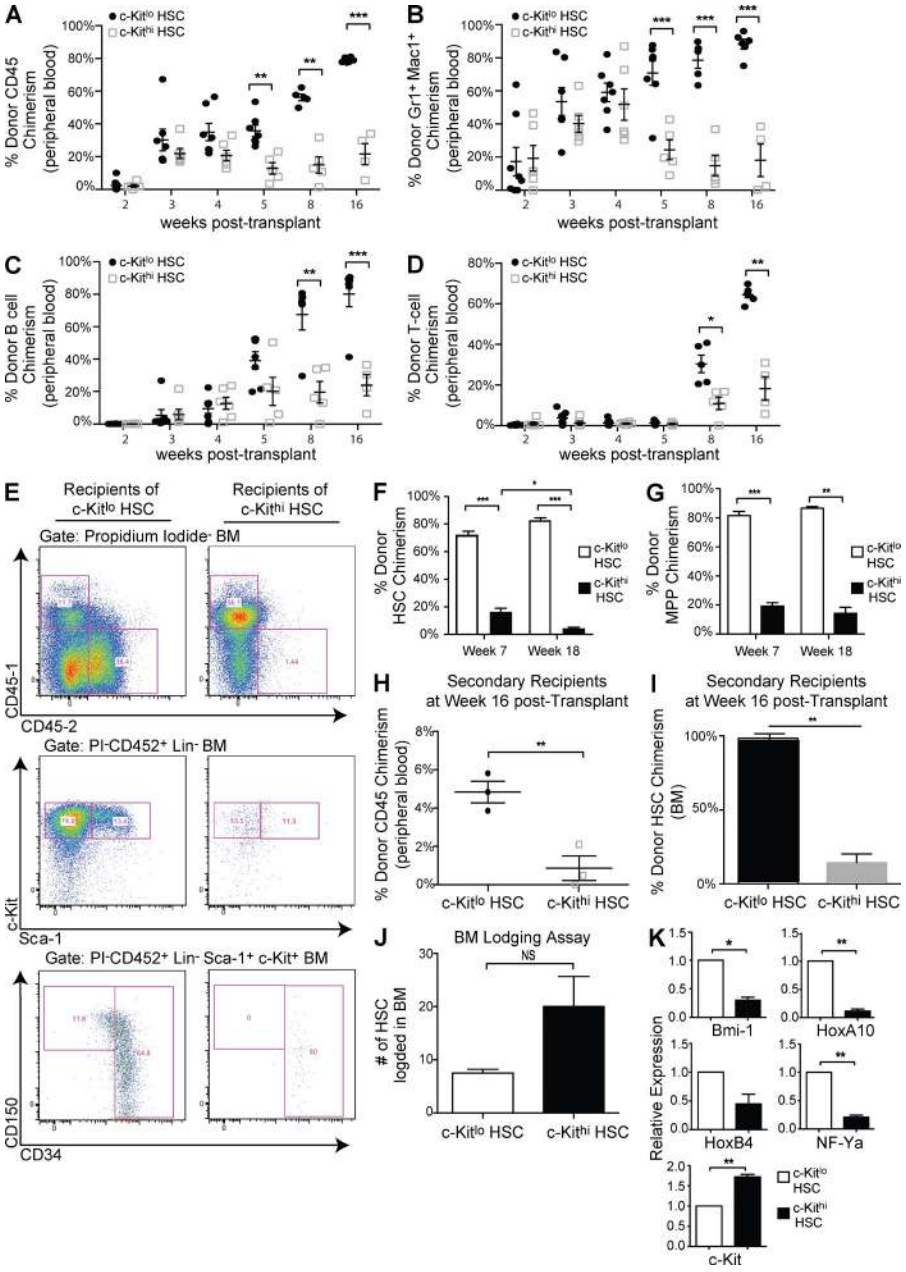

Figure 2. c-Kit^{hi} HSCs exhibit reduced engraftment potential. 400 c-Kit^{hi} and c-Kit^{lo} HSCs were double FACS-sorted from 3-mo-old C57BL/6 (CD45.2$^+$) mice and competitively transplanted into lethally irradiated C57BL/6.SJL (CD45.1$^+$) recipients with 300,000 recipient-type bone marrow cells. Donor CD45$^+$ (A), Gr1$^+$Mac1$^+$ granulocyte (B), B220$^+$ B cell (C), and CD3$^+$ T cell chimerism (D) levels were evaluated in the peripheral blood of primary recipients at the indicated time points. Each data point represents an individual recipient. (E) At week 18 after transplant, bone marrow cells from primary recipients were harvested, and donor HSC (F) and MPP ($L^-S^+K^+$ CD34$^+$; G) chimerism levels were compared with bone marrow aspirates drawn at week 7 after transplant. (H) 400 donor $L^-S^+K^+$ cells were double FACS-sorted from recipients of c-Kit^{hi} or c-Kit^{lo} HSCs and competitively transplanted into secondary, lethally irradiated recipients with 300,000 recipient-type bone marrow cells. Donor CD45 chimerism levels in the peripheral blood of secondary recipients were measured. (I) 400 donor $L^-S^+K^+$ Slam$^+$ CD34$^-$ HSCs were double-FACS sorted from an independent cohort of primary recipients that received c-Kit^{hi} or c-Kit^{lo} HSCs, and then competitively transplanted into secondary, lethally irradiated recipients with 300,000 recipient-type marrow. Donor HSC chimerism levels in the bone marrow of secondary recipients were measured. (J) 600 pCxeGFP$^+$ c-Kit^{lo} and c-Kit^{hi} HSCs were double FACS-sorted and transplanted into lethally irradiated mouse recipients. The total number of bone marrow lodged donor HSCs was evaluated 24 h after transplant. (K) qPCR of mRNA transcripts isolated from 2,000 double-sorted c-Kit^{hi} or c-Kit^{lo} HSCs. Results are representative of at least two independent experiments, and shown as mean ± SEM. n = 7–9 mice. *, $P < 0.05$; **, $P < 0.01$; ***, $P < 0.0001$.

skewed view of HSC engraftment potential. Thus, we directly assessed HSC chimerism of transplanted recipients by flow cytometry. Bone marrow aspirations performed at weeks 7 and 18 after transplant revealed stable donor HSC chimerism levels with no significant changes in mice transplanted with c-Kit^{lo} HSCs, whereas HSC chimerism significantly decreased in c-Kit^{hi} HSC-transplanted mice (Fig. 2, E and F). Similarly, mice transplanted with c-Kit^{lo} HSCs maintained high multipotent progenitor (MPP; $L^-S^+K^+$ CD34$^+$) chimerism levels, whereas MPP chimerism levels decreased in c-Kit^{hi} HSC-transplanted mice (Fig. 2 G). To evaluate the self-renewal potential of transplanted HSCs, 400 donor $L^-S^+K^+$ cells were purified from primary c-Kit^{hi} and c-Kit^{lo} HSC engrafted recipients and were transplanted into lethally irradiated secondary recipients with 300,000 competitor recipient marrow cells. 16 wk after secondary transplant, peripheral blood donor CD45 chimerism levels were 5.6-fold higher in secondary recipients transplanted with c-Kit^{lo} $L^-S^+K^+$ cells compared with c-Kit^{hi} $L^-S^+K^+$ cells ($P = 0.005$; Fig. 2 H). To confirm the difference in the self-renewal properties of c-Kit^{lo} and c-Kit^{hi} HSCs, 400 Slam$^+$ CD34$^-$ HSCs were purified from a separate cohort of primary recipients transplanted with either c-Kit^{hi} or c-Kit^{lo} HSCs, and these cells were transplanted into lethally irradiated, secondary recipients. At week 16, donor HSC chimerism levels in secondary recipients were 7.8-fold higher in recipients receiving HSCs from c-Kit^{lo} HSC primary recipients than c-Kit^{hi} HSC primary recipients ($P = 0.0013$; Fig. 2 I). These results are consistent

with the decreased in vitro colony replating activity of c-Kit^{hi} HSCs compared with c-Kit^{lo} HSCs, and confirm that c-Kit^{hi} HSCs exhibit reduced self-renewal capacity.

The mechanisms underlying the differences in long-term reconstitution capacity of c-Kit^{hi} and c-Kit^{lo} HSCs could also include deficiencies in homing to the bone marrow niche. Because the levels of peripheral blood myeloid chimerism from c-Kit^{hi} and c-Kit^{lo} HSC transplants were not significantly different in primary recipients during the first 4 wk (Fig. 2 B), these findings strongly argue against a homing deficiency. Nonetheless, to assess homing potential directly, we performed bone marrow homing assays by transplanting c-Kit^{hi} and c-Kit^{lo} HSCs into lethally irradiated recipients. Evaluation of the bone marrow 24 h later revealed no statistically significant difference in the number of c-Kit^{hi} and c-Kit^{lo} HSCs present in the bone marrow, further supporting that differential homing of c-Kit^{hi} and c-Kit^{lo} HSCs is not the reason for the observed differences in long-term engraftment (Fig. 2 J).

To better understand the molecular mechanisms underlying the functional differences between c-Kit^{lo} and c-Kit^{hi} HSCs, we evaluated the expression levels of genes previously shown to regulate HSC function. Self-renewal potential is regulated by multiple transcription factors. For instance, the loss or gain of function of Bmi-1, NF-Ya, or certain HOX family genes is associated with premature HSC exhaustion or leukemogenesis, respectively (Rizo et al., 2006). qPCR analysis of transcripts isolated from double-FACS sorted c-Kit^{hi} and c-Kit^{lo} HSCs revealed a 3 to eightfold reduction in the expression of Bmi-1, HoxA10, NF-Ya and HoxB4 (Fig. 2 K). This enrichment of genes that regulate self-renewal in c-Kit^{lo} HSCs is consistent with their increased self-renewal and engraftment potential in vivo.

c-Kit^{lo} HSCs and c-Kit^{hi} HSCs are hierarchically organized

The hematopoietic system is hierarchically organized, with HSCs differentiating into increasingly lineage committed progenitors with gradually decreasing self-renewal capacity (Pronk et al., 2007; Laurenti and Dick, 2012). Because c-Kit^{lo} HSCs exhibit significantly higher self-renewal capacity compared with c-Kit^{hi} HSCs, we hypothesized that c-Kit^{lo} HSCs are more primitive than c-Kit^{hi} HSCs and give rise to them. Assessment of c-Kit levels on c-Kit^{lo} or c-Kit^{hi} HSCs after 24 h in liquid culture revealed that 62% of c-Kit^{lo} HSCs acquired expression of c-Kit to levels comparable to those of c-Kit^{hi} HSCs before culture, whereas c-Kit^{hi} HSCs maintained their surface levels of c-Kit ($P = 0.00002$; Fig. 3, A and B). Consistent with this finding, when c-Kit^{lo} and c-Kit^{hi} HSCs were competitively transplanted and c-Kit surface levels were assessed on long-term engrafted HSCs, c-Kit expression on donor c-Kit^{lo} HSCs increased (MFI of 1,203 to 2,563; $P = 0.02$), whereas c-Kit expression levels on donor-cKit^{hi} HSCs did not significantly change (Fig. 3 C). These results are consistent with a model in which c-Kit^{lo} HSCs give rise to c-Kit^{hi} HSCs.

c-Kit^{hi} HSCs exhibit a megakaryocytic lineage bias

HSCs exhibit cell-intrinsic biases toward the lymphoid or myeloid lineages, and lineage-biased HSCs may be prospectively isolated on the basis of cell surface markers or differential drug efflux potential (Uchida et al., 2003; Dykstra et al., 2007; Weksberg et al., 2008; Beerman et al., 2010; Pang et al., 2011). Because levels of CD150 distinguish HSCs with myeloid (high CD150) or lymphoid (low CD150) biased differentiation, we measured surface CD150 levels on c-Kit^{hi} and c-Kit^{lo} HSCs, and found no difference in CD150 expression (Fig. 4 A). Consistent with this result, transplanted c-Kit^{hi} and c-Kit^{lo} HSCs produced comparable frequencies of mature lymphocytes and granulocytes/monocytes in the peripheral blood of primary recipients up to 16 wk after transplant (Fig. 4 B).

Although our in vitro assays indicated that c-Kit^{hi} HSCs give rise to increased numbers of megakaryocytes, they did not distinguish whether this was caused by increased proliferation of megakaryocyte-committed precursors or increased

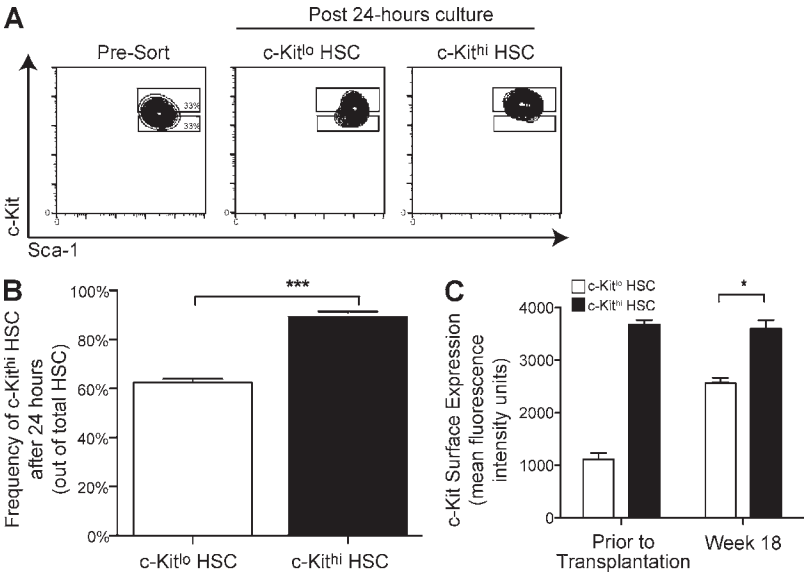

Figure 3. Hierarchical organization of c-Kit^{lo} and c-Kit^{hi} HSCs. (A) 100 c-Kit^{lo} and c-Kit^{hi} HSCs were double FACS-sorted into cytokine supplemented liquid culture using the depicted sorting gate (far left). After 24 h of culture, cells were restained and surface c-Kit expression was reevaluated to measure surface levels of c-Kit on c-Kit^{lo} (middle) and c-Kit^{hi} (far right) HSCs. (B) The frequency of c-Kit^{hi} HSCs produced by c-Kit^{lo} or c-Kit^{hi} HSCs was calculated by dividing the number of total c-Kit^{hi} HSCs in the well by the total number of HSCs remaining in each well. (C) Surface c-Kit expression on donor HSCs in recipient bone marrow at week 18 after transplant was compared with surface c-Kit expression on donor c-Kit^{hi} and c-Kit^{lo} HSCs at the time of transplant by flow cytometry. Results are representative of four independent experiments. $n = 7$ mice.

frequency of megakaryocyte-biased HSCs. Therefore, in two independent experiments we double FACS-sorted 10 single c-Kit^{lo} or c-Kit^{hi} HSCs into liquid culture and counted the number of wells containing megakaryocytes after 5 d (Fig. 4 C). c-Kit^{hi} HSCs showed a statistically significant increase in megakaryocyte production, with 45% of c-Kit^{hi} HSCs producing

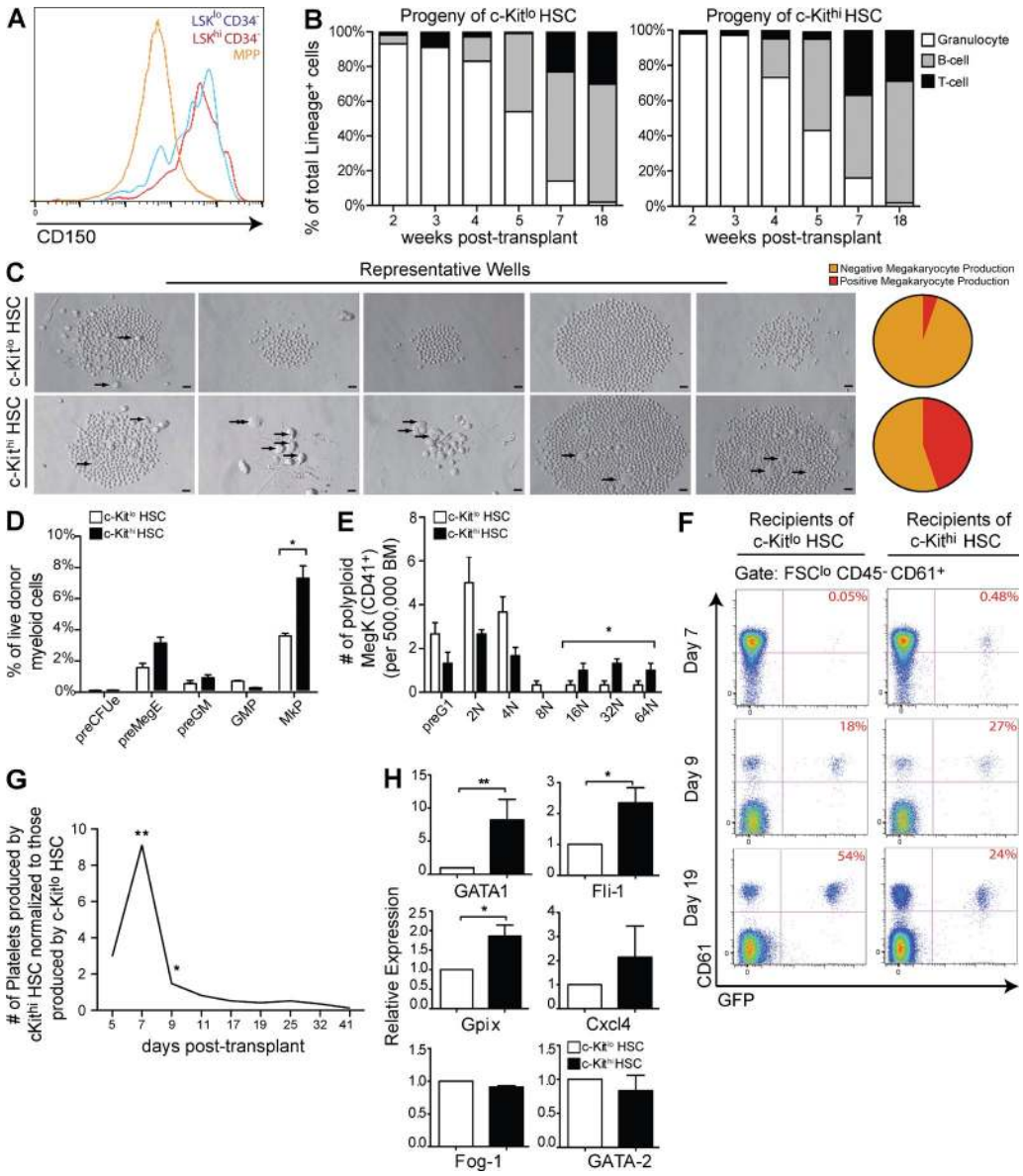

Figure 4. c-Kit^{hi} HSCs exhibit a megakaryocytic differentiation bias. (A) CD150 expression on c-Kit^{hi} and c-Kit^{lo} HSCs from freshly isolated bone marrow cells was measured by flow cytometry. (B) Donor leukocyte contributions to peripheral blood T cells (CD3^{+}), B cells (B220^{+}), and granulocytes (Gr1^{+}Mac1^{+}) was assessed by flow cytometry in mice competitively transplanted with 400 c-Kit^{hi} or c-Kit^{lo} HSCs. (C) Single c-Kit^{hi} or c-Kit^{lo} HSCs were sorted into cytokine supplemented media and the number of individual HSCs that produced megakaryocytes was evaluated 7 d later. Light microscope images of representative wells are presented with arrows indicating megakaryocytes (left). Bars, 100 µm. c-Kit^{hi} HSCs gave rise to megakaryocytes in a statistically significant manner compared with c-Kit^{lo} HSCs (P = 0.002). Graphic depiction of the frequency of individual c-Kit^{hi} and c-Kit^{lo} HSCs giving rise to megakaryocytes from two independent experiments (right). (D) Frequency of immunophenotypically defined myeloid progenitors arising from 400 c-Kit^{hi} and c-Kit^{lo} HSCs transplanted into lethally irradiated recipients 5 d after transplant. (E) Lethally irradiated mice were transplanted with 400 double-sorted GFP^{+} c-Kit^{hi} or GFP^{+} c-Kit^{lo} HSCs from pCxeGFP transgenic mice. Bone marrow of primary recipients was harvested at day 5 and 7 after transplant to evaluate early myeloid commitment and polyploid, CD41^{+} megakaryocyte maturation, respectively. (F) Donor platelet chimerism levels were evaluated in lethally irradiated mice competitively transplanted with 400 double FACS-sorted GFP^{+} c-Kit^{hi} or c-Kit^{lo} HSCs with 300,000 recipient-type bone marrow cells. Numbers shown in red represent percent donor platelet chimerism. (G) The ratio of platelet production by donor c-Kit^{hi} HSCs was normalized to that of donor c-Kit^{lo} HSC. (H) qPCR of mRNA transcripts isolated from 2,000 double-FACS sorted c-Kit^{hi} or c-Kit^{lo} HSCs. Results are representative of two to three independent experiments and are shown as mean ± SEM. *n* = 4–6 mice. *, P < 0.05; **, P < 0.01.

megakaryocytes, whereas only 5% of c-Kit^{lo} HSCs produced megakaryocytes (P = 0.002).

To confirm the in vitro megakaryocyte-biased fates of c-Kit^{hi} HSCs, we performed transplantation assays using HSCs from transgenic mice constitutively expressing GFP (pCxeGFP) to allow tracing of donor-derived platelets (Forsberg et al., 2006). Analysis of the bone marrow 5 d after transplantation of 400 HSCs and 300,000 competitor bone marrow cells into lethally irradiated mice revealed that GFP$^+$ c-Kit^{hi} HSCs produced 2-fold more preMegE progenitors and twofold more MkP than GFP$^+$ c-Kit^{lo} HSCs (P = 0.03; Fig. 4 D; Pronk et al., 2007). In addition, c-Kit^{hi} HSCs produced sixfold fewer preCFU-E progenitors. To determine if c-Kit^{hi} HSCs produced functional, platelet-forming megakaryocytes, we assessed polyploid megakaryocyte formation in the bone marrow of mice transplanted with GFP$^+$ c-Kit^{hi} or c-Kit^{lo} HSCs. At 7 d after transplant, c-Kit^{hi} HSCs produced 3.3-fold more polyploid (≥8*n*) CD41$^+$ megakaryocytes than their c-Kit^{lo} counterparts (P = 0.04; Fig. 4 E). Confirming the platelet-forming potential of HSC-derived megakaryocyte-committed progenitors as well as the more rapid differentiation kinetics of c-Kit^{hi} HSCs, transplanted c-Kit^{hi} HSCs gave rise to 9.1-fold more CD61$^+$ platelets (P = 0.006) and reached maximum platelet output 2 d earlier than c-Kit^{lo} HSCs (Fig. 4, F and G). However, c-Kit^{lo} HSCs produced 2.9-fold more platelets than c-Kit^{hi} HSCs (P = 0.06) when assessed in long-term grafts (day 66 after transplant), consistent with the impaired long-term lymphomyeloid reconstitution potential observed for c-Kit^{hi} HSCs.

To investigate the molecular basis of the functional differences between c-Kit^{hi} and c-Kit^{lo} HSCs, we measured the expression levels of genes that regulate commitment to the megakaryocytic lineage. Fli-1 binds Gata-1 and Fog-1 to coordinately regulate the expression of genes essential for megakaryocyte maturation, including Cxcl4 (Platelet Factor 4) and Gpix (Glycoprotein 9; Iwasaki et al., 2006). Gata-2 is also involved in megakaryocyte commitment, although it is most highly expressed in myelomonocytic progenitors. Consistent with their increased megakaryocytic potential, c-Kit^{hi} HSCs showed 2 to sixfold higher levels of Fli-1, Gata-1, Cxcl4, and Gpix expression than c-Kit^{lo} HSCs (Fig. 4 H). Conversely, c-Kit^{hi} HSCs expressed lower levels of Gata-2, consistent with previous observations that high levels of Gata-1 directly repress Gata-2 expression. These results indicate that c-Kit^{hi} HSCs are primed to adopt megakaryocyte lineage fates.

5-Fluorouracil (5-FU) treatment enriches for c-Kit^{lo} HSC

5-FU is a nucleotide analogue that induces death in rapidly dividing cells and therefore enriches the bone marrow for quiescent cell populations, including HSCs and immature hematopoietic progenitors (Katayama et al., 1993). Previous studies have shown that 5-FU treatment results in decreased c-Kit cell surface expression on L$^-$S$^+$K$^+$ cells, but whether or not these cells represent a specific HSC subtype was not determined (Randall and Weissman, 1997). We used 5-FU treatment to study whether stress-induced changes in c-Kit expression reflect changes in the functional composition of HSCs. As c-Kit^{hi} HSCs are more proliferative than c-Kit^{lo} HSCs, we hypothesized that 5-FU would preferentially induce apoptosis and differentiation of c-Kit^{hi} HSCs, causing a functional enrichment of c-Kit^{lo} HSCs in the marrow. To test this hypothesis, 100 c-Kit$^+$, c-Kit^{lo}, or c-Kit^{hi} HSCs were cultured in cytokine supplemented liquid culture media containing 5-FU (5ug/ml) or vehicle control. After 4 d, vehicle-treated c-Kit$^+$ and c-Kit^{lo} HSCs up-regulated c-Kit expression to levels similar to those present on c-Kit^{hi} HSCs (88 and 84%, respectively; Fig. 5 A). However, significantly fewer 5-FU–treated c-Kit$^+$ and c-Kit^{lo} HSCs up-regulated c-Kit expression to c-Kit^{hi} levels (40 and 52%, respectively; P = 0.018 and 0.05). In contrast to 5-FU–treated c-Kit$^+$ HSCs and c-Kit^{lo} HSCs, c-Kit^{hi} HSCs retained high levels of c-Kit expression, 5-FU treatment induced eightfold greater cell death in c-Kit^{hi} HSCs than c-Kit^{lo} HSCs (P = 0.014), and 5-FU–treated c-Kit^{hi} HSCs produced fivefold more L$^-$S$^-$K$^-$ and L$^-$S$^-$K$^+$ progenitors than 5-FU–treated c-Kit^{lo} HSCs and c-Kit$^+$ HSCs (P = 0.004 and 0.04, respectively; Fig. 5, B and C). Together, these data demonstrate that 5-FU does not decrease c-Kit levels on c-Kit^{hi} HSCs and that 5-FU enriches for c-Kit^{lo} HSC by preferentially inducing apoptosis and differentiation in c-Kit^{hi} HSCs.

We next determined whether the c-Kit^{lo} HSCs enriched in the bone marrow after 5-FU exhibit preserved functional properties similar to those observed in c-Kit^{lo} HSCs from mice during steady-state hematopoiesis. As mice exhibit a maximum enrichment of c-Kit^{lo} L$^-$S$^+$K$^+$ cells 3 d after 5-FU treatment (Randall and Weissman, 1997), we double FACS-sorted 10 c-Kit^{lo} or c-Kit^{hi} HSCs into cytokine-supplemented liquid culture media from mice treated with vehicle or 5-FU (167 mg/kg) at 3 d after treatment (Fig. 5 D). After 9 d in culture, c-Kit^{hi} HSCs from 5-FU–treated mice produced threefold more megakaryocytes (Lin$^-$ CD41$^+$) than c-Kit^{lo} HSCs from 5-FU–treated mice (Fig. 5 E), consistent with our finding that c-Kit^{hi} HSCs in untreated mice are megakaryocyte biased. Overall, these data demonstrate that the diminished c-Kit expression on HSCs in 5-FU–treated mice reflects changes in the functional composition of HSCs, and that the change in expression in c-Kit on HSCs in the context of 5-FU treatment is not a stochastically determined state.

Elevated c-Kit signaling is required for c-Kit^{hi} HSC function

The ability to enrich self-renewing HSCs on the basis of c-Kit expression suggests that even small changes in c-Kit signaling regulate the balance between HSC self-renewal and lineage commitment. Because SCF binding to c-Kit activates several signaling molecules involved in cell proliferation and cell fate decisions (Gotoh et al., 1996; Ryan et al., 1997), we assessed c-Kit signaling activity by measuring the levels of phosphorylated Stat5 and Stat3 in freshly isolated bone marrow by flow cytometry. Consistent with their higher levels of c-Kit signaling, c-Kit^{hi} HSCs contained a twofold higher frequency of cells expressing phosphorylated Stat5 and phosphorylated Stat3 than c-Kit^{lo} HSCs (P = 0.02 and 0.02, respectively; Fig. 6, A and B).

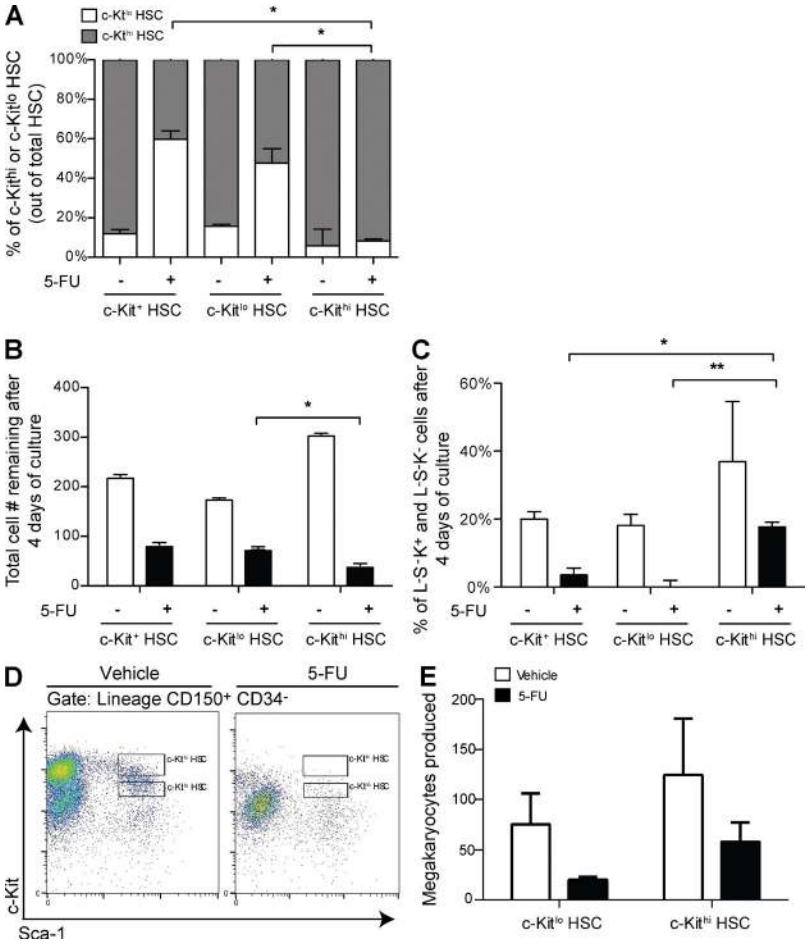

Figure 5. 5-Fluorouracil treatment preferentially eliminates c-Kit^{hi} HSCs and enriches for c-Kit^{lo} HSCs with preserved function. (A) 100 c-Kit^{lo}, c-Kit^{hi}, and total c-Kit^{+} HSCs were double FACS-sorted into cytokine-supplemented media with 5-FU or vehicle controls. The percent of c-Kit^{hi} or c-Kit^{lo} HSCs (out of total $L^{-}S^{+}K^{+}CD150^{+}CD34^{-}$ HSCs remaining in the well) was assessed after 48 h by flow cytometry. (B) Total cell counts remaining after 5-FU treatment were measured manually using a hemocytometer. (C) The frequency of mature progenitors ($L^{-}S^{-}K^{+}$ and $L^{-}S^{-}K^{-}$) cells produced after 4 d of culture was measured by flow cytometry. (D) Representative plot of c-Kit expression changes on HSCs after in vivo 5-FU treatment (167 mg/kg) at 3 d after treatment. (E) Megakaryocyte production from 10 c-Kit^{hi} and c-Kit^{lo} HSCs isolated from vehicle or 5-FU–treated mice were assessed by flow cytometry after 9 d of culture. Results are representative of two independent experiments, and shown as mean ± SEM, $n = 4$. *, $P < 0.05$; **, $P < 0.01$.

We next sought to determine if elevated levels of c-Kit signaling are required for the differentiation kinetics or megakaryocytic lineage bias of c-Kit^{hi} HSCs. We first tested whether transient inhibition of c-Kit signaling inhibits the proliferative capacity of c-Kit^{hi} HSCs by treating c-Kit^{hi} and c-Kit^{lo} HSCs cultured in cytokine-supplemented liquid culture with vehicle control or imatinib, a well-described inhibitor of c-Kit signaling (Agosti et al., 2004). To evaluate the effect of imatinib on HSCs, and not downstream progenitors, we limited imatinib exposure to 24 h, a time period during which untreated HSCs exhibit minimal proliferation with only 1 of 20 HSC dividing in that time period under similar culture conditions (unpublished data). 7 d after imatinib was removed from the media, imatinib-treated c-Kit^{hi} HSCs produced 2.7-fold fewer cells ($P < 0.05$; Fig. 6, C and D) and 3.3-fold fewer $L^{-}S^{-}K^{+}$ progenitors compared with vehicle controls (Fig. 6 E). However, imatinib treatment did not significantly affect the total cell output or differentiation of c-Kit^{lo} HSCs into $L^{-}S^{-}K^{+}$ cells.

To confirm the effect of imatinib on HSCs in vivo, mice were given daily doses of imatinib (25 mg/kg) by intraperitoneal injection for 7 d before analysis of bone marrow cells. Although imatinib treatment did not significantly affect the absolute number of common myeloid progenitors (CMPs) or granulocyte-macrophage progenitors (GMPs; Fig. 6 F), imatinib treatment did induce a 2.4-fold decrease in the absolute number of megakaryocyte/erythroid progenitors (MEPs) in comparison to vehicle-treated controls ($P = 0.04$), thereby supporting a model in which the differentiation kinetics and megakaryocyte-biased differentiation of c-Kit^{hi} HSCs depends on elevated c-Kit signaling in vivo.

To confirm that the megakaryocyte-biased differentiation of c-Kit^{hi} HSCs depends on c-Kit signaling, c-Kit^{lo} and c-Kit^{hi} HSCs were cultured in cytokine supplemented media containing titrated amounts of SCF, and the total number of megakaryocytes produced was determined by light microscopy after 5. In the absence of SCF, c-Kit^{hi} HSCs produced 5.5-fold more megakaryocytes than c-Kit^{lo} HSCs (Fig. 6 G). However, c-Kit^{hi} HSCs produced 7-, 10-, and 14-fold more megakaryocytes than c-Kit^{lo} HSCs when cultured with 0.3, 0.6, and 1.0 ng/ml of SCF, respectively, indicating that increasing concentrations of SCF preferentially induce increased megakaryocyte production in c-Kit^{hi} HSCs. Thus, megakaryocyte-biased differentiation of c-Kit^{hi} HSCs depends on c-Kit signaling.

Because imatinib is not entirely specific for c-Kit, we used a second, more specific approach to block c-Kit signaling, using a monoclonal antibody (ACK2) that binds to c-Kit

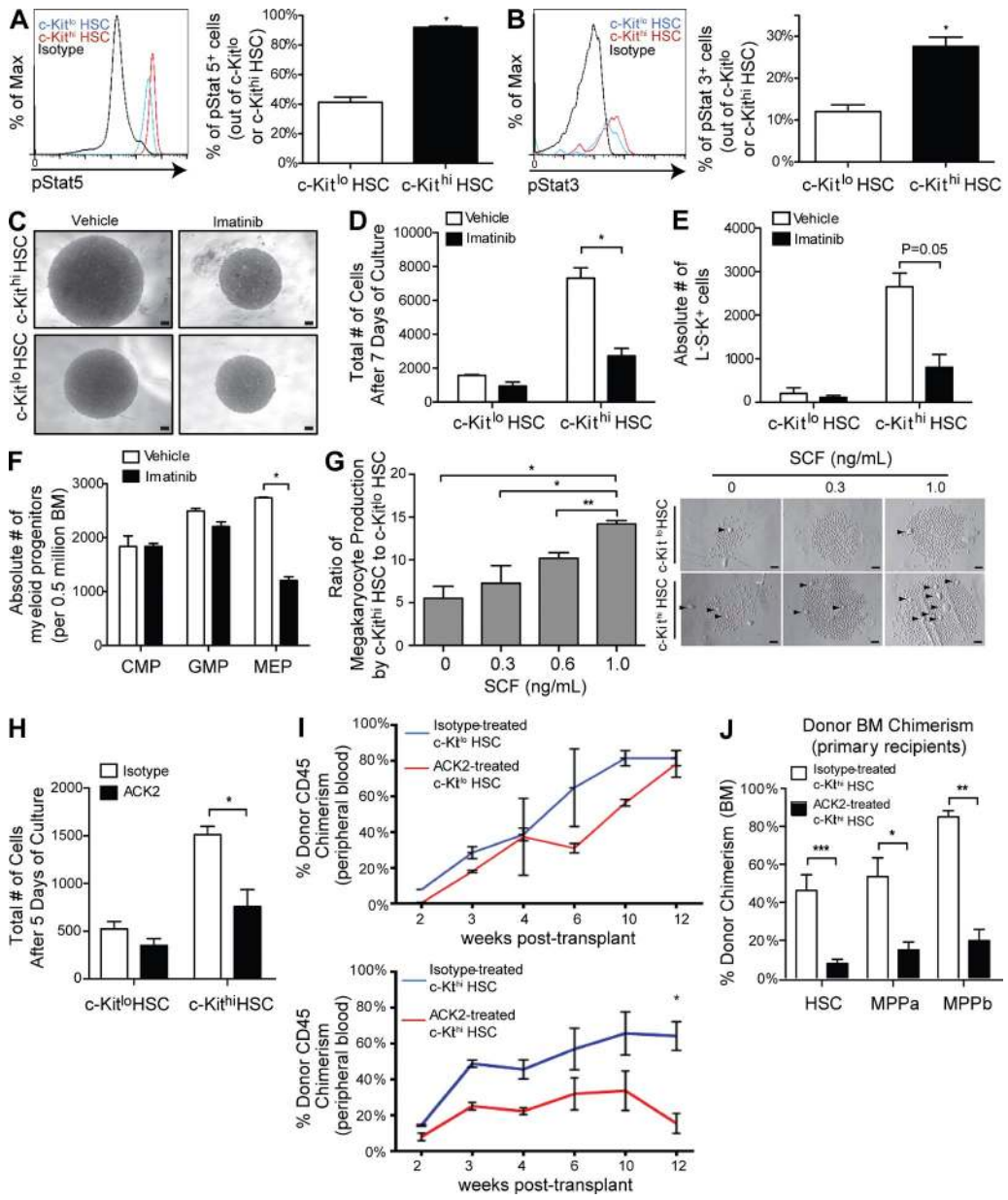

Figure 6. HSCs with differential c-Kit expression exhibit varying levels of c-Kit signaling. (A and B) Histograms of phosphorylated Stat5 and Stat3 levels in freshly isolated c-Kit^{lo} HSCs (blue), c-Kit^{hi} HSCs (red), and isotype control (orange). Frequencies of phosphorylated Stat5$^+$ or Stat3$^+$ cells among c-Kit^{hi} and c-Kit^{lo} HSCs were evaluated by flow cytometry. (C and D) 100 c-Kit^{hi} and c-Kit^{lo} HSCs were double FACS-sorted into cytokine-supplemented liquid culture and treated for 24 h with imatinib (1.0 µM) or vehicle controls, after which time cells were placed into fresh media. After 7 d of culture, total cells produced by imatinib or vehicle-treated c-Kit^{hi} and c-Kit^{lo} HSCs were measured. Bar, 400 µm. (E) Total number of L$^-$S$^-$K$^+$ progenitors produced by vehicle or imatinib-treated c-Kit^{hi} or c-Kit^{lo} HSCs was measured by flow cytometry. (F) After 7 d of daily imatinib treatment in vivo (25 mg/kg), the absolute numbers of myeloid progenitors in the bone marrow of vehicle or imatinib-treated mice were assessed using flow cytometry (CMP: Lin$^-$ c-Kit$^+$ Sca-1$^-$ CD16/32$^-$ CD34$^+$, GMP: Lin$^-$ c-Kit$^+$ Sca-1$^-$ CD16/32$^+$ CD34$^+$; MEP: Lin$^-$ c-Kit$^+$ Sca-1$^-$ CD16/32$^-$ CD34$^-$). (G) 100 c-Kit^{hi} or c-Kit^{lo} HSCs were double FACS-sorted into wells containing varying amounts of SCF ranging from 0 to 1 ng/ml. Megakaryocyte number in each well was assessed (after 5 d of megakaryocyte production) by c-Kit^{hi} HSCs normalized to that of c-Kit^{lo} HSCs (left). Light microscope images of representative wells are shown. Arrows indicate megakaryocytes (right). Bar, 100 µm. (H) 100 c-Kit^{hi} or c-Kit^{lo} HSCs were double FACs-sorted into cytokine-supplemented liquid culture and incubated with anti–c-Kit antibody (ACK2) or isotype controls. Total number of cells produced in each well was assessed manually using a hemocytometer. (I) 600 c-Kit^{hi} and c-Kit^{lo} HSCs were double FACS-sorted into cytokine-supplemented liquid culture and treated with ACK2 or isotype control for 24 h, after which they were competitively transplanted into lethally irradiated recipients (CD45.1$^+$) with 300,000 recipient-type bone marrow cells. Donor CD45 chimerism levels in the peripheral blood of mice transplanted with c-Kit^{lo} HSCs (top) or c-Kit^{hi} HSCs (bottom) were assessed at indicated time points. (J) Donor HSC chimerism levels were evaluated in bone marrow aspirates from primary recipients of isotype or ACK2-treated c-Kit^{hi} HSCs at week 12 after transplant. Results are representative of at least two independent experiments, and shown as mean ± SEM. n = 3 mice. *, $P < 0.05$; **, $P < 0.01$; ***, $P < 0.0001$.

and competes for SCF binding to determine whether c-Kit inhibition affects HSC proliferation (Shiohara et al., 1993; Czechowicz et al., 2007). Treatment of c-Kit^{hi} HSCs with ACK2 for 24 h resulted in 2.2-fold fewer cells than isotype-treated controls ($P < 0.05$), whereas ACK2 treatment did not significantly affect c-Kit^{lo} HSC proliferation (Fig. 6 H), confirming that the proliferation of c-Kit^{hi} HSCs is regulated by c-Kit signaling.

As c-Kit^{hi} and c-Kit^{lo} HSCs differed with respect to their long-term reconstitution capacities, we next evaluated whether their differences in c-Kit signaling affected their in vivo reconstitution capacity by blocking c-Kit signaling using ACK2. After incubation with ACK2 or isotype control antibody for 24 h in cytokine-supplemented media, c-Kit^{hi} or c-Kit^{lo} HSCs were transplanted with 300,000 competitor bone marrow cells into lethally irradiated mice. Mice receiving isotype-control or ACK2-treated c-Kit^{lo} HSCs exhibited similar increases in donor CD45 chimerism in the peripheral blood from week 2 to 12 after transplant (8–82% vs. 0.5–78%, respectively; Fig. 6 I, top). In contrast, although recipients of isotype control treated c-Kit^{hi} HSCs exhibited an increase in donor chimerism, recipients of ACK2-treated c-Kit^{hi} HSCs exhibited markedly lower donor chimerism during the same time period (15–57% vs. 8–15%, respectively; Fig. 6 I, bottom). Bone marrow aspirates taken at week 16 after transplant showed that donor chimerism levels of HSCs, MPPa, and MPPb in recipients of isotype-control treated c-Kit^{hi} HSCs were significantly higher than in mice transplanted with ACK2-treated c-Kit^{hi} HSCs (46 vs. 7.8%, $P = 0.005$; 54 vs.15%, $P = 0.04$; and 85 vs 20%, $P = 0.005$, respectively; Fig. 6 J). Collectively, these data demonstrate that the distinct reconstitution properties of c-Kit^{hi} HSCs depend on increased c-Kit signaling.

c-Cbl negatively regulates the transition from c-Kit^{lo} to c-Kit^{hi} HSCs

As differences in HSC function are determined by the level of c-Kit expression and signaling, we investigated the mechanisms regulating surface expression of c-Kit. Previous studies have shown that binding of SCF to c-Kit on AML cell lines results in the phosphorylation and activation of c-Cbl, an E3 ubiquitin ligase that negatively regulates SCF signaling by ubiquitinating c-Kit and stimulating internalization of activated c-Kit (Zeng et al., 2005; Masson et al., 2006). Consistent with our hypothesis that c-Cbl negatively regulates c-Kit surface expression on HSCs, c-Kit^{lo} HSCs showed 4.4-fold more phosphorylated c-Cbl^{+} cells than c-Kit^{hi} HSCs ($P = 0.02$; Fig. 7 A).

If c-Cbl negatively regulates c-Kit surface expression on HSCs, pharmacologic inhibition of c-Cbl should increase c-Kit expression on HSCs. Thus, we double-sorted c-Kit^{hi} or c-Kit^{lo} HSCs into cytokine-supplemented media and treated them with PP2, an inhibitor of Src that decreases c-Cbl phosphorylation (Zeng et al., 2005). After 24 h of treatment, PP2-treated c-Kit^{hi} HSCs did not exhibit significant changes in surface c-Kit levels compared with vehicle control, whereas c-Kit^{lo} HSCs exhibited a twofold increase in surface c-Kit MFI ($P = 0.03$), a level comparable to c-Kit^{hi} HSCs (Fig. 7 B). To confirm our observations in vivo, wild-type mice were treated with PP2 daily for 9 d. Although PP2 treatment did not increase the absolute number of c-Kit^{lo} HSCs in mice, it induced a 1.5-fold increase in the absolute number of c-Kit^{hi} HSCs, as well as a twofold increase in MkP frequency ($P = 0.002$) and 1.4-fold increase in circulating platelets ($P = 0.02$; Fig. 7, C, D, and G). These findings are consistent with a model in which c-Cbl activity negatively modulates c-Kit protein levels and suppresses the transition of c-Kit^{lo} to c-Kit^{hi} HSCs, thereby preventing megakaryocytic-biased differentiation of HSCs.

As pharmacological inhibition of c-Cbl promoted the differentiation of c-Kit^{lo} to c-Kit^{hi} HSCs, we investigated whether mice lacking c-Cbl would exhibit a similar phenotype (Zeng et al., 2005; Caligiuri et al., 2007; Rathinam et al., 2008; Naramura et al., 2010). Consistent with c-Cbl playing a negative role in megakaryocytic differentiation, 25-wk-old *c-Cbl*$^{-/-}$ mice showed 3.5-fold and 4-fold increases in the frequencies of preMegE and MkP, respectively ($P = 0.01$ and 0.03; Fig. 7, E and F). *c-Cbl*$^{-/-}$ mice also exhibited a 1.5-fold increase in circulating platelets compared with age- and sex-matched C57BL/6 (WT) controls ($P = 0.02$; Fig. 7 H). To assess whether c-Cbl deficiency alters the differentiation potential differences observed in normal HSCs defined by c-Kit expression levels, c-Kit^{hi} and c-Kit^{lo} HSCs from WT and c-Cbl$^{-/-}$ mice were cultured in cytokine supplemented medium. WT c-Kit^{hi} HSCs produced 2.9-fold more MkPs and 2.2-fold more Lin^{-} cells compared with WT c-Kit^{lo} HSCs, and c-Cbl$^{-/-}$ c-Kit^{hi} HSCs produced threefold more MkP and Lin^{-} progenitors than c-Cbl$^{-/-}$ c-Kit^{lo} HSCs after 5 d ($P = 0.002$; Fig. 7 I). Thus, c-Cbl loss did not alter the megakaryocyte-biased differentiation and differentiation kinetics of WT c-Kit^{hi} HSCs (Fig. 7 I). To test whether c-Cbl deficiency promoted the transition from c-Kit^{lo} to c-Kit^{hi} HSCs, 400 c-Kit^{lo} HSCs were double-sorted from c-Cbl$^{-/-}$ or WT mice and each population was competitively transplanted into lethally irradiated mice with 300,000 recipient-type bone marrow cells. The percentage of c-Kit^{hi} or c-Kit^{lo} HSCs produced by each donor HSC population was evaluated in bone marrow harvested from primary recipients at week 18 after transplantation. Consistent with c-Cbl negatively regulating the transition from c-Kit^{lo} to c-Kit^{hi} HSCs, mice transplanted with WT c-Kit^{lo} HSCs showed nearly equal frequencies of donor HSCs expressing c-Kit^{hi} and c-Kit^{lo} HSCs in long-term engrafted mice, whereas mice transplanted with c-Cbl$^{-/-}$ c-Kit^{lo} HSCs showed significant differences in c-Kit^{hi} and c-Kit^{lo} donor-derived HSCs with 59% c-Kit^{hi} HSCs and 8% c-Kit^{lo} HSCs ($P = 0.002$ and 0.003, respectively; Fig. 7 J).

DISCUSSION

HSCs express a unique combination of surface antigens, enabling the prospective isolation of cell populations highly enriched for long-term repopulating activity. However, genetic tracing and single-cell transplant experiments have shown that even the most highly enriched HSC populations are heterogeneous with respect to reconstitution potential, self-renewal, and lineage bias. Unfortunately, methods to prospectively

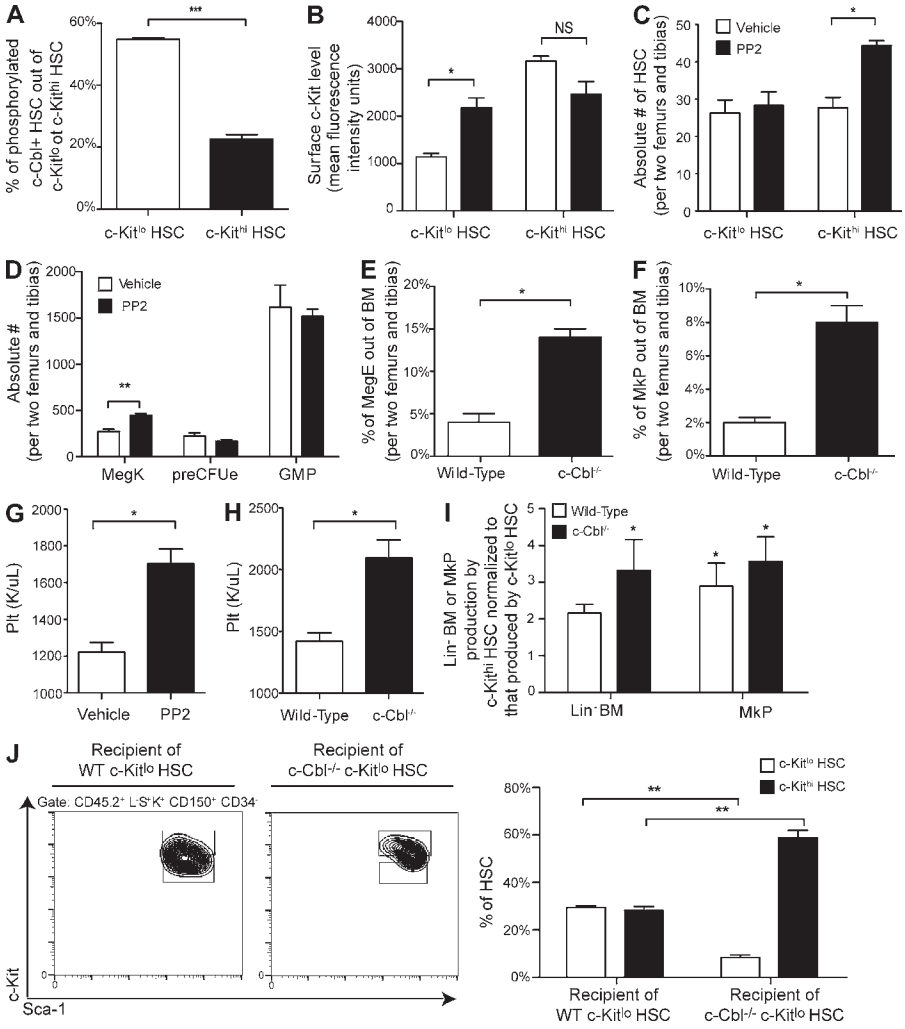

Figure 7. Loss of c-Cbl activity promotes the transition from c-Kit^{lo} to c-Kit^{hi} HSCs. (A) The level of phosphorylated c-Cbl in wild-type c-Kit^{lo} and c-Kit^{hi} HSCs was assessed by intracellular staining, followed by flow cytometry. (B) 400 c-Kit^{hi} or c-Kit^{lo} HSCs were double FACS-sorted into cytokine-supplemented liquid culture containing PP2 (0.01 M) or vehicle controls. Surface c-Kit levels were assessed by flow cytometry after 24 h of treatment. (C and D) Mice were treated daily with PP2 (5 mg/kg) or vehicle control for 9 d, and frequencies of c-Kit^{lo} HSCs, c-Kit^{hi} HSCs, and myeloid progenitors were determined per two femurs and tibias. (E and F) Frequencies of myeloid progenitors were evaluated in two femurs and tibias of c-Cbl$^{-/-}$ and WT mice. (G and H) Circulating platelet numbers were assessed in WT mice treated with PP2 or vehicle control, as well as in c-Cbl$^{-/-}$ mice using a Hemavet counter. (I) 100 WT or c-Cbl$^{-/-}$ c-Kit^{hi} or c-Kit^{lo} HSCs were sorted into media, and the production of progenitors by each cell type was assessed after 5 d. The frequency of progenitors produced by c-Kit^{hi} HSCs was normalized to the frequency produced by c-Kit^{lo} HSCs. (J) Production of donor c-Kit^{hi} HSCs was measured in mice competitively transplanted with WT or c-Cbl$^{-/-}$ c-Kit^{lo} HSCs. Results are representative of at least two independent experiments, and shown as mean ± SEM, n = 3 to 4 mice. *, $P < 0.05$; **, $P < 0.01$; ***, $P < 0.001$.

isolate such HSC subtypes are lacking, underscoring the need to develop methods to isolate functional HSC subtypes to better understand the molecular mechanisms underlying their varying biological potentials.

Although various strategies to identify long-term HSCs based on surface antigen expression have been described, almost all immunophenotypic definitions of HSCs rely on expression of c-Kit, which is a functional signaling receptor critical for maintaining HSC self-renewal and niche interactions (McCulloch et al., 1964; Maloney et al., 1978; Nakano et al., 1989; Wang and Bunting, 2008). Remarkably, despite the fact that the most highly purified HSCs exhibit a log-fold variation in expression of this receptor that is known to be critical for HSC function, relatively little effort has been devoted to investigating whether HSCs with varying c-Kit levels may represent functionally distinct HSC subtypes.

Matsuoka et al. (2011) previously demonstrated that low levels of c-Kit expression on HSCs was positively correlated with quiescent HSC cell cycle status, but they found that transplanted L$^-$S$^+$K^{lo} cells reconstituted myeloablated recipients more poorly than L$^-$S$^+$K$^+$ cells, suggesting that c-Kit^{lo} HSCs are poorer engrafters. Their latter finding stands in contradiction to our experimental results. We believe the discrepancy between the two studies is due to the use of different gating strategies to identify low c-Kit expressors, as well as the absence of CD150 and CD34 antibodies to help define HSCs in the prior study. Throughout our studies, the gate for c-Kit^{lo} HSCs was drawn to identify the population of cells that are clearly positive for c-Kit expression. In contrast, Matsuoka et al. (2011) drew their low c-Kit gate to include cells that are low to negative for c-Kit, likely introducing significant contamination of their LSK gate with non-HSC-like cells (Fig. S2). The differing conclusions drawn by the Matsuoka et al. (2011) study and ours are likely due to differences in the cell populations transplanted. Indeed, our analysis of L$^-$S$^+$K^{lo} cells using our gating strategy for c-Kit expression reveals a relative enrichment of HSCs (Lin$^-$c-Kit$^+$Sca-1$^+$CD34$^-$SLAM$^+$) in comparison to Matsuoka et al.'s population of L$^-$S$^+$K^{lo} cells, which were significantly enriched with non-HSCs (Fig. S2). Using a more highly enriched population of HSCs defined by their Lin$^-$c-Kit$^+$Sca-1$^+$CD34$^-$SLAM$^+$ immunophenotype, we show that these long-term HSCs can be fractionated into

c-Kit^{hi} and c-Kit^{lo} populations and that HSCs expressing high levels of c-Kit exhibit significantly reduced long-term and serial engraftment capacities and are megakaryocyte-biased. These functional differences were confirmed by decreased expression of transcripts encoding self-renewal genes in c-Kit^{hi} HSCs. Moreover, we show that c-Kit^{lo} and c-Kit^{hi} HSCs are hierarchically organized, with c-Kit^{lo} HSCs giving rise to c-Kit^{hi} HSCs, but not vice versa, as demonstrated through both in vitro differentiation assays and serial transplantation experiments in vivo. Based on the developmental relationship between c-Kit^{lo} and c-Kit^{hi} HSCs, the significant differences in their long-term reconstitution potential in both primary and secondary transplants, and the functional evidence that c-Kit signaling activity mediates the different functional outputs of c-Kit^{lo} and c-Kit^{hi} HSCs, we believe that the preponderance of evidence supports a model in which our immunophenotypically defined c-Kit^{lo} HSCs are the most primitive HSCs most enriched for self-renewing HSCs.

Our studies also provide functional evidence using multiple approaches to support a direct role of c-Kit signaling in mediating the differential functions observed within Lin$^-$c-Kit$^+$Sca-1$^+$CD34$^-$SLAM$^+$ HSCs. First, c-Kit^{hi} HSCs exhibit elevated levels of c-Kit signaling as demonstrated by higher levels of intracellular phosphorylated Stat5 and Stat3, both known downstream mediators of c-Kit signaling. Second, inhibition of c-Kit signaling in c-Kit^{hi} or c-Kit^{lo} HSCs using either inhibitors or blocking antibodies affected the engraftment potential and lineage-biased differentiation of c-Kit^{hi} HSCs, but not c-Kit^{lo} HSCs. Together, these data indicate that lower levels of c-Kit surface expression and their reduced signaling identify HSCs that are enriched for long-term reconstitution capacity and self-renewal.

HSCs with high or low levels of CD150 exhibit biased differentiation toward the myeloid or lymphoid lineage, respectively (Beerman et al., 2010), and HSCs with lower or upper side-population rhodamine staining are enriched for CD150^{hi} myeloid-biased cells or CD150^{lo} lymphoid-biased cells, respectively (Challen et al., 2010). Here, we show that c-Kit^{hi} and c-Kit^{lo} HSCs expressed similar levels of CD150, and that they produced a similar distribution of B-cells, T cells, and granulocytes in the peripheral blood of primary recipients; thus, the differences in c-Kit^{hi} and c-Kit^{lo} HSC function is not due to differences in CD150 expression. In addition, c-Kit^{hi} HSCs preferentially developed into megakaryocytes, an intrinsic lineage-bias present at the level of the HSC that was not previously identified by differential CD150 or rhodamine staining. As c-Kit^{hi} HSCs also exhibit increased cell cycling, these results are consistent with recent data that described heightened expression of megakaryocyte genes among nonquiescent, long-term HSCs. Based on the rapid differentiation kinetics and expression of key megakaryocyte genes in c-Kit^{hi} HSCs, we speculate that c-Kit^{hi} HSCs likely are rapidly recruited to expand and give rise to megakaryocytic precursors during emergency thrombopoiesis. It would be interesting to determine whether c-Kit^{hi} HSCs are preferentially expanded in other situations associated with high platelet production, such as acute blood loss, or in myeloproliferative disorders associated with high platelet counts.

Our data support a model in which c-Kit surface expression and signaling levels are finely regulated to ensure the proper balance between HSC self-renewal and non–self-renewing cell divisions associated with commitment to the megakaryocytic lineage. For example, although the distribution of c-Kit expression on HSCs changes under condition of stress such as 5-FU treatment, the functional differences between c-Kit^{hi} and c-Kit^{lo} HSCs are largely preserved under these conditions. In addition, c-Kit expression levels are conserved in c-Kit^{hi} and c-Kit^{lo} HSCs after transplantation, confirming the association between c-Kit expression levels and stable HSC functional subtypes. Thus, c-Kit levels appear to be regulated to assure proper HSC responses to physiological stimuli. Although our data support a model in which, tonic or low levels of c-Kit activity are required for long-term HSC maintenance in the normal, wild-type setting, it is clear that markedly attenuated c-Kit signaling can be deleterious and results in HSC loss, as demonstrated by loss-of-function c-Kit mutants and ACK2-treated c-Kit^{hi} HSCs. Thus, consistent with our findings of preserved function of HSCs based on c-Kit expression levels in the context of 5-FU treatment. HSCs require finely tuned levels of c-Kit signaling to maximize their self-renewal properties.

The E3 ubiquitin ligase c-Cbl was previously described as a potential regulator of c-Kit signaling by promoting degradation of active c-Kit receptors in AML cell lines (Zeng et al., 2005); however, its potential role in regulating c-Kit in vivo was not described previously, despite the description of the *c-Cbl*$^{-/-}$ mouse myeloproliferative phenotype (Rathinam et al., 2010). Using orthogonal approaches, our experimental data are consistent with a model in which c-Cbl is a negative regulator of c-Kit in HSCs and therefore promotes self-renewal and nonmegakaryocyte biased hematopoietic differentiation. Pharmacological inhibition of c-Cbl with PP2 increased surface c-Kit levels in c-Kit^{lo} HSCs, and in vivo treatment of PP2 increased the frequencies of c-Kit^{hi} HSCs, MkPs, and platelets. Moreover, c-Cbl–deficient c-Kit^{lo} HSCs produced significantly higher frequencies of c-Kit^{hi} HSCs than WT c-Kit^{lo} HSCs in the transplantation setting, supporting a critical role of c-Cbl in the transition from c-Kit^{lo} to c-Kit^{hi} HSCs. Though these studies highlight a new function of c-Cbl in the regulation of HSC subtype composition, we suspect that a complex orchestration of cell-intrinsic factors and microenvironmental factors may also regulate c-Kit stability and/or activity, possibly through the generation of membrane-bound and soluble SCF by cells that make up the bone marrow microenvironment. Such studies directed at dissecting the relative contributions of cell intrinsic or extrinsic-mediated signals in regulating HSC c-Kit levels in both homeostatic and stress conditions will yield important new insights regarding the mechanisms that regulate the functional heterogeneity and composition of HSCs.

MATERIALS AND METHODS

Mice and transplantations. C57BL/6 and C57BL/6.SJL mice were purchased from The Jackson Laboratory. All recipient mice were conditioned for

transplantation with lethal irradiation (9.5 Gy) using a cesium source. 12 h after irradiation, cells for transplants were injected intravenously into the retroorbital sinus of recipient mice under isoflurane anesthesia. Irradiated mice were provided with antibiotics (Sulfatrim) for 5 wk after transplantation. Tetracycline-inducible, GFP-tagged histone 2B transgenic (TetOP-H2B-GFP) mice were a gift from H. Hock (Harvard Medical School, Boston, MA). H2B-GFP expression was induced by providing mice with drinking water containing doxycycline (MP 198955; 2 mg/ml) for at least 6 wk. pCxeGFP transgenic mice have been previously described (Wright et al., 2001; Forsberg et al., 2006), and were a gift from I. Weissman (Stanford University, Stanford, CA). All mice were maintained under pathogen-free conditions according to an MSKCC IACUC-approved protocol.

Bone marrow analysis/cell purification. Bone marrow cells were harvested by crushing two tibias, two femurs, two pelvises, and one spine from each mouse. Bone marrow cells were enriched for immature cells using anti–mouse CD117 MicroBeads and an autoMACS machine (both Miltenyi Biotec) per manufacturer's instructions. c-Kit–enriched populations were stained with antibodies against lineage markers (B220, CD3, Gr-1, Mac-1, and Ter119), c-Kit, Sca-1, CD150, CD16/32, and CD34 (eBioscience) as previously described (McGowan et al., 2011). Stained samples were either analyzed or sorted using a FACSAria II (BD). For all experiments in which c-Kit^{hi} or c-Kit^{lo} HSCs were purified, they were double-sorted to ensure >95% purity. To calculate the frequency of hematopoietic precursors, two femurs and two tibias were flushed into 1x PBS containing 2.5% fetal calf serum (Hyclone). Bone marrow aspirations were performed on mice under isoflurane anesthesia per IACUC-approved protocol. Aspirates were treated with ACK lysis buffer and stained in PBS/2.5% fetal calf serum with antibodies against lineage markers, c-Kit, Sca-1, CD150, CD16/32, Flk2, CD34, CD48, and CD41 for analysis on hematopoietic stem and progenitor cells. For myeloid progenitors, bone marrow cells were stained with antibodies against lineage markers, c-Kit, Sca-1, CD150, CD16/32, CD41, CD105, and CD71, as described by Pronk et al. (2007).

In vitro culture assay. For liquid culture studies, cells were double FACS-sorted into cytokine-supplemented media composed of DMEM/F12 (CellGro), 10% fetal calf serum, Pen/Strep (Invitrogen), Glutamax (Invitrogen), IL-3, IL-6, TPO, EPO, GM-CSF, SCF, and Flt3 (all cytokines from PeproTech), as previously described (McGowan et al., 2011). Total cell counts of each well were performed using a hemocytometer. For methylcellulose assays, sorted cells were grown in complete methylcellulose media (Stem Cell Technologies; M3434) and colonies were scored at the indicated time points.

For single-cell analysis of megakaryocyte production, 20 single HSCs from the c-Kit^{lo} and c-Kit^{hi} HSC fractions were double-FACS sorted into individual wells containing cytokine supplemented liquid culture media, and the wells were evaluated at the indicated time points. Statistical significance was calculated based on an assumption of a binomial distribution for megakaryocyte production for both c-Kit^{lo} and c-Kit^{hi} HSCs.

Peripheral blood analysis. Peripheral blood samples were collected in 50 mM EDTA solution (Thermo Fisher Scientific) via lateral tail vein incision. Dextran was then added to the cells for a final concentration of 2% and incubated for 40 min at 37°C. Cells collected from dextran-treated samples were then incubated with red blood cell lysis buffer (ACK). Cells were then washed once with PBS/2.5% fetal calf serum, and then cells were resuspended and then stained in PBS/2.5% fetal calf serum with antibodies against Ter119, CD3, B220, Gr-1, Mac-1, CD61, CD45.2, and CD45.1 for chimerism studies. Blood samples for platelet analysis were not treated with Dextran.

Intracellular staining. Harvested bone marrow cells were stained in PBS/2.5% fetal calf serum containing 500 μM vanadate (Sigma-Aldrich). Cells were fixed with 1.5% formaldehyde for 30 min at room temperature and permeabilized with ice-cold, 100% methanol for 10 min on ice. Intracellular antigens were stained using antibodies against phosphorylated Stat5 and phosphorylated Stat3 (BD) for 30 min on ice.

ACK2, imatinib, and 5-FU treatment. Sorted cells were incubated with imatinib (1.0 μM in <1% DMSO solution), the anti–c-Kit antibody ACK2 (eBioscience), isotype control (10 μg/ml), 5-FU (5 ng/ml), or vehicle (<1% DMSO in PBS) in cytokine-supplemented liquid culture (described above). For in vivo studies, mice were injected intraperitoneally with imatinib (25 mg/kg) or vehicle daily.

Cell cycle analysis. Bone marrow cells were stained with the LIVE/DEAD stain according to manufacturer instructions (Invitrogen). Hematopoietic stem and progenitor populations were identified by staining with antibodies as described above. For cell cycle analysis, cells were fixed and permeabilized using a kit provided by eBioScience, and were stained with an antibody against Ki67 (BD Biosciences) and Hoechst 33342 (Invitrogen) for 30 min at room temperature immediately before flow cytometric analysis.

Megakaryocyte ploidy staining. Bone marrow cells were harvested and stained with LIVE/DEAD stain (Invitrogen). After cells were incubated with antibodies against CD41, c-Kit, and CD150, they were fixed and permeabilized according to manufacturer protocols (eBioScience). Nuclear DNA content was determined by staining with Hoechst 33342 for 30 min at room temperature immediately before flow cytometric analysis.

qPCR. mRNA from 2,000 double FACS-sorted populations of c-Kit^{hi} and c-Kit^{lo} HSC from 16-wk-old C57BL/6 mice was isolated using TRIzol (Invitrogen). Transcripts were reverse transcribed according to manufacturer protocols (Invitrogen), and qPCR was performed using SYBR Green (Applied Biosystems). GAPHD transcript levels were used for normalization. Primer sequences were determined using Primer3 Design Tool. Sequences for probes used include the following: HoxA10, 5′-GGAAGCATGGACATTCAGGT-3′ and 5′-CCAGGCAAGCAAGACCTTAG-3′; NF-Ya, 5′-AGTAGGGGAGAGCAGCCTTC-3′ and 5′-CTAGCATGTGGGCAGACAGA-3′; Cxcl4, 5′-GGGCAGGCAGTGAAGATAAA-3′ and 5′-GATCTCCATCGCTTTCTTCG-3′; Gpix, 5′-GTACCTGCCAGTCCTTGGAA-3′ and 5′-GGGTTGTGTGTCACATCCAG-3′; Itga2b, 5′-AAGCTCTGAGCACACCCACT-3′ and 5′-CTCAGCCCTTCACTCTGACC-3′; Fli-1, 5′-ACTTGACCAGGGTTGGTCTG-3′ and 5′-CTGCCCATTGTGAGGAATTT-3′; Gata-1, 5′-GATGGAATCCAGACGAGGAA-3′ and 5′-GCCCTGACAGTACCACAGGT-3′; Bmi-1, 5′-TGTCCAGGTTCACAAAACCA-3′ and 5′-TGCAACTTCTCCTCGGTCTT-3′; Gata-2, 5′-ACCACCCTTGATGTCCATGT-3′ and 5′-TGCATGCAAGAGAAGTCACC-3′; Fog-1, 5′-TGCTATATGTGCGCCTTGTC-3′ and 5′-TTGATGACTGCGGTAGCAAG-3′; GAPDH, 5′-AACTTTGGCATTGTGGAAGG-3′ and 5′-ACACATTGGGGGTAGGAACA-3′.

Online supplemental material. Fig. S1 shows the gating method used to define c-Kit^{lo} and c-Kit^{hi} HSCs. Fig. S2 is a comparison of different gating strategies to identify c-Kit positive cells. Online supplemental material is available at http://www.jem.org/cgi/content/full/jem.20131128/DC1.

We would like to thank Drs. Omar Abdel-Wahab, Peter Besmer, Michael Kharas, and Ross Levine for helpful discussion and advice.

The authors have no competing financial interests to declare.

Submitted: 30 May 2013
Accepted: 31 December 2013

REFERENCES

Agosti, V., S. Corbacioglu, I. Ehlers, C. Waskow, G. Sommer, G. Berrozpe, H. Kissel, C.M. Tucker, K. Manova, M.A. Moore, et al. 2004. Critical role for Kit-mediated Src kinase but not PI 3-kinase signaling in pro T and pro B cell development. *J. Exp. Med.* 199:867–878. http://dx.doi.org/10.1084/jem.20031983

Beerman, I., D. Bhattacharya, S. Zandi, M. Sigvardsson, I.L. Weissman, D. Bryder, and D.J. Rossi. 2010. Functionally distinct hematopoietic stem cells modulate hematopoietic lineage potential during aging by a mechanism of clonal expansion. *Proc. Natl. Acad. Sci. USA.* 107:5465–5470. http://dx.doi.org/10.1073/pnas.1000834107

Bosbach, B., S. Deshpande, F. Rossi, J.H. Shieh, G. Sommer, E. de Stanchina, D.R. Veach, J.M. Scandura, K. Manova-Todorova, M.A. Moore, et al. 2012. Imatinib resistance and microcytic erythrocytosis in a KitV558Δ;T669I/+ gatekeeper-mutant mouse model of gastrointestinal stromal tumor. *Proc. Natl. Acad. Sci. USA*. 109:E2276–E2283. http://dx.doi.org/10.1073/pnas.1115240109

Bryder, D., D.J. Rossi, and I.L. Weissman. 2006. Hematopoietic stem cells: the paradigmatic tissue-specific stem cell. *Am. J. Pathol.* 169:338–346. http://dx.doi.org/10.2353/ajpath.2006.060312

Caligiuri, M.A., R. Briesewitz, J. Yu, L. Wang, M. Wei, K.J. Arnoczky, T.B. Marburger, J. Wen, D. Perrotti, C.D. Bloomfield, and S.P. Whitman. 2007. Novel c-CBL and CBL-b ubiquitin ligase mutations in human acute myeloid leukemia. *Blood*. 110:1022–1024. http://dx.doi.org/10.1182/blood-2006-12-061176

Challen, G.A., N.C. Boles, S.M. Chambers, and M.A. Goodell. 2010. Distinct hematopoietic stem cell subtypes are differentially regulated by TGF-beta1. *Cell Stem Cell*. 6:265–278. http://dx.doi.org/10.1016/j.stem.2010.02.002

Christensen, J.L., and I.L. Weissman. 2001. Flk-2 is a marker in hematopoietic stem cell differentiation: a simple method to isolate long-term stem cells. *Proc. Natl. Acad. Sci. USA*. 98:14541–14546. http://dx.doi.org/10.1073/pnas.261562798

Czechowicz, A., D. Kraft, I.L. Weissman, and D. Bhattacharya. 2007. Efficient transplantation via antibody-based clearance of hematopoietic stem cell niches. *Science*. 318:1296–1299. http://dx.doi.org/10.1126/science.1149726

Dykstra, B., D. Kent, M. Bowie, L. McCaffrey, M. Hamilton, K. Lyons, S.J. Lee, R. Brinkman, and C. Eaves. 2007. Long-term propagation of distinct hematopoietic differentiation programs in vivo. *Cell Stem Cell*. 1:218–229. http://dx.doi.org/10.1016/j.stem.2007.05.015

Forsberg, E.C., T. Serwold, S. Kogan, I.L. Weissman, and E. Passegué. 2006. New evidence supporting megakaryocyte-erythrocyte potential of flk2/flt3+ multipotent hematopoietic progenitors. *Cell*. 126:415–426. http://dx.doi.org/10.1016/j.cell.2006.06.037

Foudi, A., K. Hochedlinger, D. Van Buren, J.W. Schindler, R. Jaenisch, V. Carey, and H. Hock. 2009. Analysis of histone 2B-GFP retention reveals slowly cycling hematopoietic stem cells. *Nat. Biotechnol.* 27:84–90. http://dx.doi.org/10.1038/nbt.1517

Gerrits, A., B. Dykstra, O.J. Kalmykowa, K. Klauke, E. Verovskaya, M.J. Broekhuis, G. de Haan, and L.V. Bystrykh. 2010. Cellular barcoding tool for clonal analysis in the hematopoietic system. *Blood*. 115:2610–2618. http://dx.doi.org/10.1182/blood-2009-06-229757

Glimm, H., I.H. Oh, and C.J. Eaves. 2000. Human hematopoietic stem cells stimulated to proliferate in vitro lose engraftment potential during their S/G(2)/M transit and do not reenter G(0). *Blood*. 96:4185–4193.

Gotoh, A., H. Takahira, C. Mantel, S. Litz-Jackson, H.S. Boswell, and H.E. Broxmeyer. 1996. Steel factor induces serine phosphorylation of Stat3 in human growth factor-dependent myeloid cell lines. *Blood*. 88:138–145.

Iwasaki, H., S. Mizuno, Y. Arinobu, H. Ozawa, Y. Mori, H. Shigematsu, K. Takatsu, D.G. Tenen, and K. Akashi. 2006. The order of expression of transcription factors directs hierarchical specification of hematopoietic lineages. *Genes Dev.* 20:3010–3021. http://dx.doi.org/10.1101/gad.1493506

Katayama, N., J.P. Shih, S. Nishikawa, T. Kina, S.C. Clark, and M. Ogawa. 1993. Stage-specific expression of c-kit protein by murine hematopoietic progenitors. *Blood*. 82:2353–2360.

Kiel, M.J., O.H. Yilmaz, T. Iwashita, O.H. Yilmaz, C. Terhorst, and S.J. Morrison. 2005. SLAM family receptors distinguish hematopoietic stem and progenitor cells and reveal endothelial niches for stem cells. *Cell*. 121:1109–1121. http://dx.doi.org/10.1016/j.cell.2005.05.026

Laurenti, E., and J.E. Dick. 2012. Molecular and functional characterization of early human hematopoiesis. *Ann. N. Y. Acad. Sci.* 1266:68–71. http://dx.doi.org/10.1111/j.1749-6632.2012.06577.x

Maloney, M.A., M.J. Dorie, R.A. Lamela, Z.R. Rogers, and H.M. Patt. 1978. Hematopoietic stem cell regulatory volumes as revealed in studies of the bgj/bgj:W/WV chimera. *J. Exp. Med.* 147:1189–1197. http://dx.doi.org/10.1084/jem.147.4.1189

Masson, K., E. Heiss, H. Band, and L. Rönnstrand. 2006. Direct binding of Cbl to Tyr568 and Tyr936 of the stem cell factor receptor/c-Kit is required for ligand-induced ubiquitination, internalization and degradation. *Biochem. J.* 399:59–67. http://dx.doi.org/10.1042/BJ20060464

Matsuoka, Y., Y. Sasaki, R. Nakatsuka, M. Takahashi, R. Iwaki, Y. Uemura, and Y. Sonoda. 2011. Low level of c-kit expression marks deeply quiescent murine hematopoietic stem cells. *Stem Cells*. 29:1783–1791. http://dx.doi.org/10.1002/stem.721

McCulloch, E.A., L. Siminovitch, and J.E. Till. 1964. Spleen-Colony Formation in Anemic Mice of Genotype Ww. *Science*. 144:844–846. http://dx.doi.org/10.1126/science.144.3620.844

McGowan, K.A., W.W. Pang, R. Bhardwaj, M.G. Perez, J.V. Pluvinage, B.E. Glader, R. Malek, S.M. Mendrysa, I.L. Weissman, C.Y. Park, and G.S. Barsh. 2011. Reduced ribosomal protein gene dosage and p53 activation in low-risk myelodysplastic syndrome. *Blood*. 118:3622–3633. http://dx.doi.org/10.1182/blood-2010-11-318584

Miller, C.L., V.I. Rebel, M.E. Lemieux, C.D. Helgason, P.M. Lansdorp, and C.J. Eaves. 1996. Studies of W mutant mice provide evidence for alternate mechanisms capable of activating hematopoietic stem cells. *Exp. Hematol.* 24:185–194.

Morita, Y., H. Ema, and H. Nakauchi. 2010. Heterogeneity and hierarchy within the most primitive hematopoietic stem cell compartment. *J. Exp. Med.* 207:1173–1182. http://dx.doi.org/10.1084/jem.20091318

Müller-Sieburg, C.E., R.H. Cho, M. Thoman, B. Adkins, and H.B. Sieburg. 2002. Deterministic regulation of hematopoietic stem cell self-renewal and differentiation. *Blood*. 100:1302–1309.

Nakano, T., N. Waki, H. Asai, and Y. Kitamura. 1989. Lymphoid differentiation of the hematopoietic stem cell that reconstitutes total erythropoiesis of a genetically anemic W/Wv mouse. *Blood*. 73:1175–1179.

Naramura, M., N. Nandwani, H. Gu, V. Band, and H. Band. 2010. Rapidly fatal myeloproliferative disorders in mice with deletion of Casitas B-cell lymphoma (Cbl) and Cbl-b in hematopoietic stem cells. *Proc. Natl. Acad. Sci. USA*. 107:16274–16279. http://dx.doi.org/10.1073/pnas.1007575107

Pang, W.W., E.A. Price, D. Sahoo, I. Beerman, W.J. Maloney, D.J. Rossi, S.L. Schrier, and I.L. Weissman. 2011. Human bone marrow hematopoietic stem cells are increased in frequency and myeloid-biased with age. *Proc. Natl. Acad. Sci. USA*. 108:20012–20017. http://dx.doi.org/10.1073/pnas.1116110108

Passegué, E., A.J. Wagers, S. Giuriato, W.C. Anderson, and I.L. Weissman. 2005. Global analysis of proliferation and cell cycle gene expression in the regulation of hematopoietic stem and progenitor cell fates. *J. Exp. Med.* 202:1599–1611. http://dx.doi.org/10.1084/jem.20050967

Pietras, E.M., M.R. Warr, and E. Passegué. 2011. Cell cycle regulation in hematopoietic stem cells. *J. Cell Biol.* 195:709–720. http://dx.doi.org/10.1083/jcb.201102131

Pronk, C.J., D.J. Rossi, R. Månsson, J.L. Attema, G.L. Norddahl, C.K. Chan, M. Sigvardsson, I.L. Weissman, and D. Bryder. 2007. Elucidation of the phenotypic, functional, and molecular topography of a myeloerythroid progenitor cell hierarchy. *Cell Stem Cell*. 1:428–442. http://dx.doi.org/10.1016/j.stem.2007.07.005

Randall, T.D., and I.L. Weissman. 1997. Phenotypic and functional changes induced at the clonal level in hematopoietic stem cells after 5-fluorouracil treatment. *Blood*. 89:3596–3606.

Rathinam, C., C.B. Thien, W.Y. Langdon, H. Gu, and R.A. Flavell. 2008. The E3 ubiquitin ligase c-Cbl restricts development and functions of hematopoietic stem cells. *Genes Dev.* 22:992–997. http://dx.doi.org/10.1101/gad.1651408

Rathinam, C., C.B. Thien, R.A. Flavell, and W.Y. Langdon. 2010. Myeloid leukemia development in c-Cbl RING finger mutant mice is dependent on FLT3 signaling. *Cancer Cell*. 18:341–352. http://dx.doi.org/10.1016/j.ccr.2010.09.008

Rizo, A., E. Vellenga, G. de Haan, and J.J. Schuringa. 2006. Signaling pathways in self-renewing hematopoietic and leukemic stem cells: do all stem cells need a niche? *Hum. Mol. Genet.* **15**(Spec No 2, Spec No 2):R210–R219. http://dx.doi.org/10.1093/hmg/ddl175

Ryan, J.J., H. Huang, L.J. McReynolds, C. Shelburne, J. Hu-Li, T.F. Huff, and W.E. Paul. 1997. Stem cell factor activates STAT-5 DNA binding in IL-3-derived bone marrow mast cells. *Exp. Hematol.* 25:357–362.

Sharma, Y., C.M. Astle, and D.E. Harrison. 2007. Heterozygous kit mutants with little or no apparent anemia exhibit large defects in overall

hematopoietic stem cell function. *Exp. Hematol.* 35:214–220. http://dx.doi.org/10.1016/j.exphem.2006.10.001

Shiohara, M., K. Koike, T. Kubo, Y. Amano, M. Takagi, K. Muraoka, J. Nakao, T. Nakahata, and A. Komiyama. 1993. Possible role of stem cell factor as a serum factor: monoclonal anti-c-kit antibody abrogates interleukin-6-dependent colony growth in serum-containing culture. *Exp. Hematol.* 21:907–912.

Thorén, L.A., K. Liuba, D. Bryder, J.M. Nygren, C.T. Jensen, H. Qian, J. Antonchuk, and S.E. Jacobsen. 2008. Kit regulates maintenance of quiescent hematopoietic stem cells. *J. Immunol.* 180:2045–2053.

Uchida, N., B. Dykstra, K.J. Lyons, F.Y. Leung, and C.J. Eaves. 2003. Different in vivo repopulating activities of purified hematopoietic stem cells before and after being stimulated to divide in vitro with the same kinetics. *Exp. Hematol.* 31:1338–1347.

van der Wath, R.C., A. Wilson, E. Laurenti, A. Trumpp, and P. Liò. 2009. Estimating dormant and active hematopoietic stem cell kinetics through extensive modeling of bromodeoxyuridine label-retaining cell dynamics. *PLoS ONE.* 4:e6972. http://dx.doi.org/10.1371/journal.pone.0006972

Wang, Z., and K.D. Bunting. 2008. Hematopoietic stem cell transplant into non-myeloablated W/Wv mice to detect steady-state engraftment defects. *Methods Mol. Biol.* 430:171–181. http://dx.doi.org/10.1007/978-1-59745-182-6_12

Waskow, C., V. Madan, S. Bartels, C. Costa, R. Blasig, and H.R. Rodewald. 2009. Hematopoietic stem cell transplantation without irradiation. *Nat. Methods.* 6:267–269. http://dx.doi.org/10.1038/nmeth.1309

Weksberg, D.C., S.M. Chambers, N.C. Boles, and M.A. Goodell. 2008. CD150- side population cells represent a functionally distinct population of long-term hematopoietic stem cells. *Blood.* 111:2444–2451. http://dx.doi.org/10.1182/blood-2007-09-115006

Wilson, A., E. Laurenti, G. Oser, R.C. van der Wath, W. Blanco-Bose, M. Jaworski, S. Offner, C.F. Dunant, L. Eshkind, E. Bockamp, et al. 2008. Hematopoietic stem cells reversibly switch from dormancy to self-renewal during homeostasis and repair. *Cell.* 135:1118–1129. http://dx.doi.org/10.1016/j.cell.2008.10.048

Wilson, A., E. Laurenti, and A. Trumpp. 2009. Balancing dormant and self-renewing hematopoietic stem cells. *Curr. Opin. Genet. Dev.* 19:461–468. http://dx.doi.org/10.1016/j.gde.2009.08.005

Wright, D.E., S.H. Cheshier, A.J. Wagers, T.D. Randall, J.L. Christensen, and I.L. Weissman. 2001. Cyclophosphamide/granulocyte colony-stimulating factor causes selective mobilization of bone marrow hematopoietic stem cells into the blood after M phase of the cell cycle. *Blood.* 97:2278–2285. http://dx.doi.org/10.1182/blood.V97.8.2278

Yee, N.S., I. Paek, and P. Besmer. 1994. Role of kit-ligand in proliferation and suppression of apoptosis in mast cells: basis for radiosensitivity of white spotting and steel mutant mice. *J. Exp. Med.* 179:1777–1787. http://dx.doi.org/10.1084/jem.179.6.1777

Zeng, S., Z. Xu, S. Lipkowitz, and J.B. Longley. 2005. Regulation of stem cell factor receptor signaling by Cbl family proteins (Cbl-b/c-Cbl). *Blood.* 105:226–232. http://dx.doi.org/10.1182/blood-2004-05-1768